

# The Real Topological String on a local Calabi-Yau

Daniel Kreff<sup>a,b</sup> and Johannes Walcher<sup>b</sup>

<sup>a</sup> *Arnold Sommerfeld Center for Theoretical Physics, LMU Munich, Germany*

<sup>b</sup> *PH-TH Division, CERN, Geneva, Switzerland*

## Abstract

We study the topological string on local  $\mathbb{P}^2$  with O-plane and D-brane at its real locus, using three complementary techniques. In the A-model, we refine localization on the moduli space of maps with respect to the torus action preserved by the anti-holomorphic involution. This leads to a computation of open and unoriented Gromov-Witten invariants that can be applied to any toric Calabi-Yau with involution. We then show that the full topological string amplitudes can be reproduced within the topological vertex formalism. We obtain the real topological vertex with trivial fixed leg. Finally, we verify that the same results derive in the B-model from the extended holomorphic anomaly equation, together with appropriate boundary conditions. The expansion at the conifold exhibits a gap structure that belongs to a so far unidentified universality class.

February 2009

# Contents

<b>1</b>	<b>Introduction and Overview</b>	<b>2</b>
<b>2</b>	<b>The A-model</b>	<b>8</b>
2.1	Localization . . . . .	8
2.2	Orientifolded localization . . . . .	11
<b>3</b>	<b>The real topological vertex</b>	<b>17</b>
3.1	Topological vertex for local $\mathbb{P}^2$ . . . . .	18
3.2	Taking a squareroot . . . . .	19
<b>4</b>	<b>The B-model</b>	<b>21</b>
4.1	Solving the (extended) holomorphic anomaly equations . . . . .	22
4.2	Fixing the holomorphic ambiguities . . . . .	25
<b>5</b>	<b>Conclusion</b>	<b>31</b>
	<b>Acknowledgments</b>	<b>32</b>
<b>A</b>	<b>Real Gopakumar-Vafa invariants of local <math>\mathbb{P}^2</math></b>	<b>32</b>
	<b>References</b>	<b>36</b>

## 1 Introduction and Overview

There has been a lot of progress in closed and open topological string theory in the last couple of years. The improved understanding concerns in particular local (non-compact) backgrounds defined by toric Calabi-Yau manifolds together with toric branes on top. While many lessons were learned (for reviews see for instance [1, 2]), it has long not been clear how they would apply to compact backgrounds, which indeed remain the challenging case to understand in general.

Recently, it has become clearer that there are significant qualitative distinctions between the non-compact and compact settings. Perhaps the most dramatic additional ingredient is a topological analogue [3] of the tadpole cancellation condition familiar from the type II superstring. In particular, a satisfactory BPS interpretation of the topological string amplitudes requires that one consider topological string orientifolds, whose charge precisely cancels that of the background D-branes. We will be considering

O-planes and D-branes defined via the fixed locus of an anti-holomorphic involution, and will refer to the resulting theory as the real topological string.

Issues such as tadpole cancellation might seem to cast doubt on the general applicability of any local lessons. As an example, large- $N$  dualities cannot be useful if the total D-brane charge is restricted. In the present paper, we show that the situation is actually slightly better. Specifically, we will study the real topological string on the local Calabi-Yau manifold given by the canonical bundle over the projective plane (local  $\mathbb{P}^2$ ). Among our main findings are several parallels both with the usual toric story, as well as with the real topological string on a compact manifold. We hope that these connections will prove useful for both lines of investigation.

A physical motivation for the importance of the real topological string comes from considering the combined open and closed type IIA superstring with orientifold projection, which is a well-known playground for string phenomenology. Recall that this orientifold projection is the gauging of a discrete symmetry  $I \circ P$ , where  $I$  is an anti-holomorphic involution of the internal background  $X$  and  $P$  denotes parity reversal on the string world-sheet. The world-sheets of the orientifolded theory then have general topology, in the sense that they can be oriented or unoriented and may possess boundaries and/or cross-caps. As is well known, one can represent these world-sheets as quotients  $\hat{\Sigma}/\sigma$  of a closed oriented world-sheet  $\hat{\Sigma}$  by an anti-holomorphic involution  $\sigma$ . The equivalence class of  $\sigma$  determines the topology of  $\hat{\Sigma}/\sigma$ . In the non-perturbative (in  $\alpha'$ ) sector of such orientifolded type IIA theories, one has to consider world-sheet instantons with general topology, *i.e.*, maps from Riemann surfaces with or without boundaries and cross-caps into target-space equipped with involution. As usual, the summation of world-sheet instantons is best done by considering the topological theory, which is the interest of the present paper.

We begin by recalling the main features of the setup of [3], and fix some notation, before summarizing our main results.

The target space that we shall study is the local Calabi-Yau  $X = \mathcal{O}_{\mathbb{P}^2}(-3)$ . The involution  $I$  defining the orientifold projection is simply complex conjugation. The fixed point locus,  $L$ , on which we shall wrap one D-brane, is the real version of the canonical bundle, and can be thought of as the real line bundle defined by the orientation bundle over  $\mathbb{R}\mathbb{P}^2$ . (Note that, as special Lagrangian,  $L$ , itself, is oriented.)

The central object to compute is the total, or combined open-closed-unoriented<sup>1</sup>

---

<sup>1</sup>To emphasize one point again: When the tadpole cancelling D-branes are put right on top of

topological string free energy, which in a perturbative expansion can be written as:

$$\mathcal{G} = \sum_{\chi=-2}^{\infty} \mathcal{G}^{(\chi)} \lambda^{\chi}, \quad (1.1)$$

Here  $\mathcal{G}^{(\chi)}$  is the contribution at order  $\chi$ , and  $\lambda$  is the string coupling. In general, the  $\mathcal{G}$  and  $\mathcal{G}^{(\chi)}$  depend on closed and open string moduli, which in the A-model consist of Kähler moduli of  $X$  and complexified Wilson lines on the D-branes. In the example of interest, we have  $H_2(X; \mathbb{Z}) = \mathbb{Z}$ , and  $H_1(L; \mathbb{Z}) = \mathbb{Z}_2$ , so we have one continuous closed string modulus, denoted by  $t \equiv \log q$ , and one discrete open string modulus,  $\epsilon = \pm 1$ . Thus,

$$\mathcal{G}^{(\chi)} = \mathcal{G}^{(\chi)}(t, \epsilon). \quad (1.2)$$

On general grounds, one expects to be able to compute  $\mathcal{G}^{(\chi)}$  by summing contributions from individual world-sheet topologies,<sup>2</sup>

$$\mathcal{G}^{(\chi)} = \sum_{2g+h-2=\chi} \mathcal{F}^{(g,h)} + \sum_{2g+h-1=\chi} \mathcal{R}^{(g,h)} + \sum_{2g+h-2=\chi} \mathcal{K}^{(g,h)}. \quad (1.3)$$

Namely,  $\mathcal{F}^{(g,h)}$  (with  $\mathcal{F}^{(g)} \equiv \mathcal{F}^{(g,0)}$ ) is the contribution of oriented genus  $g$  surfaces with  $h$  boundaries,  $\mathcal{R}^{(g,h)}$  is the contribution of unoriented genus  $g$  surfaces with  $h$  boundaries and an odd number of cross-caps (note that one can trade three cross-caps for a handle plus a cross-cap) and  $\mathcal{K}^{(g,h)}$  comes from unoriented genus  $g$  surfaces with  $h$  boundaries and an even number of cross-caps. (Note that one can trade two cross-caps for a Klein handle, that is a handle with orientation reversal. The genus  $g$  in  $\mathcal{K}^{(g,h)}$  refers to the number of handles plus the number of Klein handles, with at least one Klein handle.)

Moreover, each of those contributions in (1.3) should be computable by counting the number of maps from the appropriate surfaces into the background, similar to the expansion of the closed string free energy

$$\mathcal{F} = \sum_{g=0}^{\infty} \mathcal{F}^{(g)} \lambda^{2g-2}, \quad (1.4)$$

---

the orientifold plane, we refer to the theory as “real”. Certain of the present definitions are good somewhat more generally.

<sup>2</sup>In contrast to the physically motivated normalization of  $\mathcal{G}^{(\chi)}$  used in [3], we chose here a different normalization which is more convenient for practical computations.

with (ignoring constant map contributions polynomial in  $t = \log q$ )

$$\mathcal{F}^{(g)} = \sum_d \tilde{n}_d^{(g)} q^d, \quad (1.5)$$

where the sum is over (positive)  $d \in H_2(X; \mathbb{Z})$ , and  $\tilde{n}_d^{(g)}$  are the rational Gromov-Witten invariants. For future reference, we note the following expansion of  $\mathcal{F}$  in terms of integer BPS degeneracies, *i.e.*, Gopakumar-Vafa invariants  $N_d^{(g)}$ ,

$$\mathcal{F} = \sum_{g,d,k} N_d^{(g)} \frac{1}{k} \left( 2 \sinh \frac{\lambda k}{2} \right)^{2g-2} q^{kd}. \quad (1.6)$$

In hindsight (say if one is given the answer by some other means) it is not necessarily clear how to disentangle the individual contributions in (1.3). Cancellation of the O-plane tadpole allows wrapping only a single D-brane on  $L$ , so we only have one discrete open string modulus  $\epsilon$  at our disposal. This only allows distinguishing whether  $h$  is even or odd. In some of our computations, however, there are ways to effectively introduce arbitrary numbers of brane-antibrane pairs, each with their discrete Wilson line degree of freedom. This allows keeping track of individual world-sheet topologies. Then we may write for  $h > 0$ :

$$\begin{aligned} \mathcal{F}^{(g,h)} &= \sum_{d \equiv h \pmod{2}} \tilde{n}_d^{(g,h)} q^{d/2} \epsilon^h, \\ \mathcal{K}^{(g,h)} &= \sum_{d \equiv h \pmod{2}} \tilde{n}_d^{(g,h)_k} q^{d/2} \epsilon^h, \end{aligned} \quad (1.7)$$

where the  $\tilde{n}_d^{(g,h)}$  and  $\tilde{n}_d^{(g,h)_k}$  are appropriate open and unoriented Gromov-Witten invariants. In these expressions,  $d$  refers to the relative homology class in  $H_2(X, L)$ , or in the case of unoriented surfaces, the homology class of the covering map.

More precisely, to write (1.7), one has to assume a certain prescription to deal with homologically trivial boundaries, which we will recall below. This prescription, together with the map  $H_2(X, L) \rightarrow H_1(L)$  also explains the restriction to  $d \equiv h \pmod{2}$ , and entails the vanishing of the  $\mathcal{R}^{(g,h)}$  in our model.

Independently of such assumptions, we can isolate the contribution from purely oriented closed strings (because that is known from before the orientifold projection!). Thus we define the amplitude  $\mathcal{G}'^{(\chi)}$

$$\mathcal{G}'^{(\chi)} = \mathcal{G}^{(\chi)} - \begin{cases} \mathcal{F}^{(\frac{\chi}{2}+1,0)} & \text{for } \chi \text{ even} \\ 0 & \text{for } \chi \text{ odd} \end{cases}, \quad (1.8)$$

which can be seen to have an expansion of the form

$$\mathcal{G}'^{(\chi)} = \sum_{d \equiv \chi \pmod{2}} n_d'^{(\chi)} q^{d/2} \epsilon^\chi, \quad (1.9)$$

in terms of rational numbers  $n_d'^{(\chi)}$ , which one might call real Gromov-Witten invariants. As found in [3], the combined open-closed-unoriented topological string free energy without oriented closed string contribution,

$$\mathcal{G}' = \sum_{\chi} \mathcal{G}'^{(\chi)} \lambda^\chi, \quad (1.10)$$

possesses an expansion with integer coefficients  $N_d'^{(\chi)}$ , similar to that of the  $\mathcal{F}^{(g)}$  in eq. (1.6)

$$\frac{1}{2} \mathcal{G}' = \sum_{\substack{d \equiv \chi \pmod{2} \\ k \text{ odd}}} N_d'^{(\chi)} \frac{1}{k} \left( 2 \sinh \frac{\lambda k}{2} \right)^\chi q^{kd/2} \epsilon^\chi. \quad (1.11)$$

The  $N_d'^{(\chi)}$  should be seen as a real version of Gopakumar-Vafa invariants, counting real degree  $d$  curves. Physically, they also count dimensions of Hilbert spaces of appropriate BPS objects [4].

A nice property of the real topological string is that local and compact backgrounds are more closely related (the real brane is usually non-toric in local settings), and hence one can learn more for the compact case from the local real case than from the usual toric open topological string. On the other hand, some calculation techniques from the local toric case remain applicable, as we will explain presently.

For the model at hand, the individual contributions in (1.7) can be explicitly calculated via localization on the moduli space of stable maps, as performed by Kontsevich to calculate  $\tilde{n}_d^{(0)}$  [5], generalized by several authors to the open string case [6, 7] and recently completed by the inclusion of unoriented strings [3]. Especially, localization was used to compute various oriented amplitudes for our model of interest, *i.e.*, local  $\mathbb{P}^2$ , in [8, 9]. The essential point that allows the extension to the real case, in this and other models, is that although the real brane is usually non-toric, it is often left invariant by the action of at least a one-dimensional torus. This is enough for localization to apply. (A toric brane in the usual sense is by definition always invariant under a two-dimensional torus.) We will review and apply this approach in section 2 to calculate the individual contributions to the topological amplitudes of local  $\mathbb{P}^2$  for some higher  $\chi$  and  $d$ .

In section 3, we will take a different approach to the same problem and derive the total topological string amplitudes via a real version of the topological vertex. Recall that the standard topological vertex solves the closed topological string (with background toric branes) on local toric Calabi-Yau threefolds by evaluating a certain cubic field theory on the toric diagram of the Calabi-Yau viewed as a Feynman diagram [10]. Applications of the topological vertex to orientifolds have been considered before, such as in [11, 12]. In these works, the involution defining the orientifold was taken to be freely acting. The main new feature in our study is that we deal with a non-empty orientifold plane. This also requires the introduction of a specific D-brane into the background on top of the O-plane. An orientifold model that can be solved with these techniques of either localization or the topological vertex has the property that the toric diagram has an involutive symmetry to define the orientifold projection. (Toric Calabi-Yaus, which are rigid, are always invariant under complex conjugation, but unless this can be dressed with a symmetry of the toric diagram, no toric symmetry will be preserved.) There are then several possible cases for the fixed point locus. A new feature arises when there are vertices fixed under the involution of the toric diagram, and one then has to distinguish whether the fixed leg (of which there is necessarily exactly one) ending on the fixed vertex is “external” to the toric diagram or not. We will call the requisite transition amplitude the “real topological vertex”. By studying real local  $\mathbb{P}^2$ , we will be able to deduce the real vertex in which the fixed leg is external. Since our main aim here is a proof of principle, we will not try to go beyond that. It is conceivable that a more complete theory exists.

Both localization and the topological vertex fail in general for compact models. The only tool available which works also in the compact setup, is mirror symmetry together with the (extended) holomorphic anomaly equations of [13, 14]. This approach has the notorious problem that one has to fix the holomorphic ambiguity (boundary conditions on moduli space) at each order in perturbation theory. In the closed topological string it has been shown [15, 16] that detailed information about the singularity structure at the conifold locus can be carried over to compact models and leads to a very efficient solution scheme up to very high genus. For non-compact models, the same structure leads to complete integrability (for an explicit example, see [17]). It is natural to look for a similar structure also in the real topological string, and indeed we will make a find, see section 4.

Mirror symmetry and the holomorphic anomaly have the advantage that they give

an answer to all orders in the instanton expansion, but the disadvantage that they are limited to an order-by-order calculation in the string coupling expansion. On the other hand, the topological vertex gives an all-order result in the string coupling, but in practical computations is limited to the first few orders in the instanton expansion. Finally, localization is an order-by-order computation in both directions, and also computationally rather challenging. What it has going for it is that of the three techniques we study, it is the one that is likely easiest to put on a rigorous mathematical foundation.

Some more concluding words with a sketch of possible directions of follow-up research are offered in section 5. Finally, the results for the real Gopakumar-Vafa invariants  $N_d^{r(x)}$  of local  $\mathbb{P}^2$  are collected in appendix A.

## 2 The A-model

In this section, we explain the computation of open and unoriented Gromov-Witten invariants of the real topological string on local  $\mathbb{P}^2$  using localization on the space of maps. For the reader's convenience, we firstly recall some basics about the localization calculation for pure closed string world-sheets. A more detailed exposition can be found in standard textbooks on mirror symmetry or in the original works [5, 18]. We then discuss the extension to open and unoriented world-sheets developed in [3]. Especially, we will work out in more detail some technical issues which are important at higher degree and genus. Some actual results of our calculations are listed in appendix A. The reader not interested in explicit A-model computations may safely skip this section.

### 2.1 Localization

We first briefly recall the basics of how to calculate the pure oriented closed string contribution  $\tilde{n}_d^{(g,0)}$  for local  $\mathbb{P}^2$  via localization.

Define  $\overline{\mathcal{M}}_d^{\hat{\Sigma}} \equiv \overline{\mathcal{M}}_{\hat{g},0}(d, \mathbb{P}^2)$  as the moduli space of stable maps  $\hat{f} : \hat{\Sigma} \rightarrow \mathbb{P}^2$  from genus  $\hat{g}$  curves into  $\mathbb{P}^2$  with image of degree  $d \in H_2(\mathbb{P}^2, \mathbb{Z})$ . Let  $\mathbf{e}(\mathcal{E}_d)$  be the Euler class of the bundle  $\mathcal{E}_d = H^1(\Sigma^g, f^*\mathcal{O}(-3))$  over  $\overline{\mathcal{M}}_d^{\hat{\Sigma}}$ . Then, the Gromov-Witten invariants  $\tilde{n}_d^{\hat{\Sigma}} \equiv \tilde{n}_d^{(\hat{g},0)}$  are given by

$$\tilde{n}_d^{\hat{\Sigma}} = \int_{\overline{\mathcal{M}}_d^{\hat{\Sigma}}} \mathbf{e}(\mathcal{E}_d). \quad (2.1)$$

These integrals can be evaluated by the Atiyah-Bott localization formula.



To this end, consider the  $\hat{\mathbb{T}} = (\mathbb{C}^*)^3$  group action on  $\mathbb{P}^2$ . The fixed points of  $\hat{\mathbb{T}}$  on  $\mathbb{P}^2$  are the three points  $p_i$  given by the projectivization of the  $i$ -th coordinate line of  $\mathbb{C}^3$ . The only curves invariant under  $\hat{\mathbb{T}}$  are the three lines  $l_{ij}$  joining the  $p_i$ . The  $\hat{\mathbb{T}}$  action can be pulled back to an action on  $\overline{\mathcal{M}}_d^{\hat{\Sigma}}$ . We will denote the  $\hat{\mathbb{T}}$ -invariant subspace of  $\overline{\mathcal{M}}_d^{\hat{\Sigma}}$  as  $\hat{\mathbb{T}}\overline{\mathcal{M}}_d^{\hat{\Sigma}}$ . Since a point in  $\hat{\mathbb{T}}\overline{\mathcal{M}}_d^{\hat{\Sigma}}$  is a map of a genus  $\hat{g}$  curve  $\hat{\Sigma}$  to the  $\hat{\mathbb{T}}$ -invariant locus in  $\mathbb{P}^2$ , we immediately deduce that  $\hat{\Sigma}$  can only consist of the union of a certain number of  $n_v$ -pointed irreducible genus  $g_v$  curves  $C_{v,n_v}^{(g_v)}$  joined together by 2-pointed spheres. The  $C_{v,n_v}^{(g_v)}$  are contracted to one of the three points  $p_i$ , while the spheres are mapped to the  $l_{ij}$ . It follows that each map  $\hat{f}$  can be represented combinatorially as a connected graph, *i.e.*, to each map  $\hat{f}$  we associate a graph  $\hat{\Gamma}$  by identifying each contracted component of  $\hat{\Sigma}$  with a decorated vertex, where the decoration is given by the genus of the component and the point  $p_i$  it maps to in target space. The spheres joining the contracted components are then identified with edges joining the corresponding vertices, where each edge is decorated with the degree (*i.e.*, the multi-cover) of the map which sends the corresponding sphere to  $l_{ij}$ .

Thus, we have a map which associates to each point in  $\hat{\mathbb{T}}\overline{\mathcal{M}}_d^{\hat{\Sigma}}$  a decorated graph. Note that the map is not one-to-one, but rather each graph  $\hat{\Gamma}$  corresponds to a subspace  $\hat{M}_d^{\hat{\Gamma}} \subset \hat{\mathbb{T}}\overline{\mathcal{M}}_d^{\hat{\Sigma}}$ .

In order to see this, observe that each vertex of the graph  $\hat{\Gamma}$  comes with the moduli space of an  $n_v$ -pointed genus  $g_v$  curve, usually denoted as  $\overline{\mathcal{M}}_{g_v, n_v}$ . Hence, each graph corresponds to the moduli space  $\overline{\mathcal{M}}_{\hat{\Gamma}}$  given by

$$\overline{\mathcal{M}}_{\hat{\Gamma}} = \prod_v \overline{\mathcal{M}}_{g_v, val(v)} . \quad (2.2)$$

Obviously, there exists a map  $\gamma_{\hat{\Gamma}} : \overline{\mathcal{M}}_{\hat{\Gamma}} \rightarrow \hat{M}_d^{\hat{\Gamma}}$ , which is however not an isomorphism. In order to obtain an isomorphism, we need to quotient by the automorphism group of  $\overline{\mathcal{M}}_{\hat{\Gamma}}$  given by  $\mathbb{A}_{\hat{\Gamma}} = \text{Aut}(\hat{\Gamma}) \times \prod_e \mathbb{Z}_{d_e}$ , where  $\text{Aut}(\hat{\Gamma})$  is the automorphism group of  $\hat{\Gamma}$  as a decorated graph.

Thus, we have

$$\hat{\mathbb{T}}\overline{\mathcal{M}}_d^{\hat{\Sigma}} \cong \bigcup_{\hat{\Gamma}} (\overline{\mathcal{M}}_{\hat{\Gamma}} / \mathbb{A}_{\hat{\Gamma}}) , \quad (2.3)$$

where the union is over the set of all non-isomorphic graphs  $\hat{\Gamma}$  whose topology and decoration fulfill the following criteria:

- $\sum_e d_e = d$ .

- $1 - |v| + |e| + \sum_v g_v = \hat{g}$ , where  $|v|$  and  $|e|$  is the number of vertices and edges, respectively.
- $i(v_a) \neq i(v_b)$ , for  $v_a$  connected to  $v_b$ , where  $i(v_j)$  encodes the point in target space the corresponding component maps to.

Applying the Atiyah-Bott localization formula then tells us that we can evaluate (2.1) via a sum over graphs:

$$\tilde{n}_d^{\hat{\Sigma}} = \sum_{\hat{\Gamma}} \frac{1}{|\mathbb{A}_{\hat{\Gamma}}|} \int_{\mathcal{M}_{\hat{\Gamma}}} \frac{\mathbf{e}(i^* \mathcal{E}_d)}{\mathbf{e}(\mathcal{N}_{\hat{\Gamma}}^{vir})} , \quad (2.4)$$

where  $|\mathbb{A}_{\hat{\Gamma}}|$  is the order of the group  $\mathbb{A}_{\hat{\Gamma}}$ .

Explicit expressions for  $\mathbf{e}(i^* \mathcal{E}_d)$  and  $\mathbf{e}(\mathcal{N}_{\hat{\Gamma}}^{vir})$  in equivariant cohomology have been derived in [18]. We restate them here for convenience:

$$\mathbf{e}(i^* \mathcal{E}_d) = \prod_v \lambda_{i(v)}^{val(v)-1} P_{g(v)}(\Lambda_{i(v)}) \prod_e \prod_{m=1}^{3d_e-1} \left[ \Lambda_{i(e)} + \frac{m}{d_e} (\lambda_{i(e)} - \lambda_{j(e)}) \right] , \quad (2.5)$$

$$\begin{aligned} \frac{1}{\mathbf{e}(\mathcal{N}_{\hat{\Gamma}}^{vir})} &= \prod_e \frac{(-1)^{d_e} d_e^{2d_e}}{(d_e!)^2 (\lambda_{i(e)} - \lambda_{j(e)})^{2d_e}} \prod_{\substack{k \neq i(e), j(e) \\ a=0}}^{d_e} \frac{1}{\frac{a}{d_e} \lambda_{i(e)} + \frac{d_e-a}{d_e} \lambda_{j(e)} - \lambda_k} \\ &\times \prod_v \prod_{j \neq i(v)} (\lambda_{i(v)} - \lambda_j)^{val(v)-1} \\ &\times \begin{cases} \prod_v \left[ (\sum_F w_F^{-1})^{val(v)-3} \prod_{F \ni v} w_F^{-1} \right] & \text{for } g(v) = 0 \\ \prod_v \prod_{j \neq i(v)} P_{g(v)}(\lambda_{i(v)} - \lambda_j) \prod_{F \ni v} \frac{1}{w_F - \kappa_F} & \text{for } g(v) \geq 1 \end{cases} , \end{aligned} \quad (2.6)$$

with

$$\begin{aligned} w_F &= (\lambda_{i(F)} - \lambda_{j(F)}) / d_e , \\ \Lambda_i &= \lambda_1 + \lambda_2 + \lambda_3 - 3\lambda_i , \\ P_g(x) &= \sum_{r=0}^g c_{g-r}(E^*) x^r , \end{aligned} \quad (2.7)$$

where  $i(e)$  and  $j(e)$  refer to the target space points the vertices attached to the edge  $e$  map to,  $F$  runs over the set of flags of a vertex, that is, all pairs  $(v, e)$  for a fixed vertex  $v$  with  $e$  ending on  $v$ . For a flag, we have  $i(F) = i(v)$  and  $j(F)$  refers to the other end point of  $e$ . Finally,  $E$  is the Hodge bundle,  $\kappa_F$  is a gravitational descendant and  $\lambda_i$  are the torus weights.

Thus, the integration in equation (2.4) boils down to the evaluation of Hodge integrals, for which one can use Faber's algorithm [19].

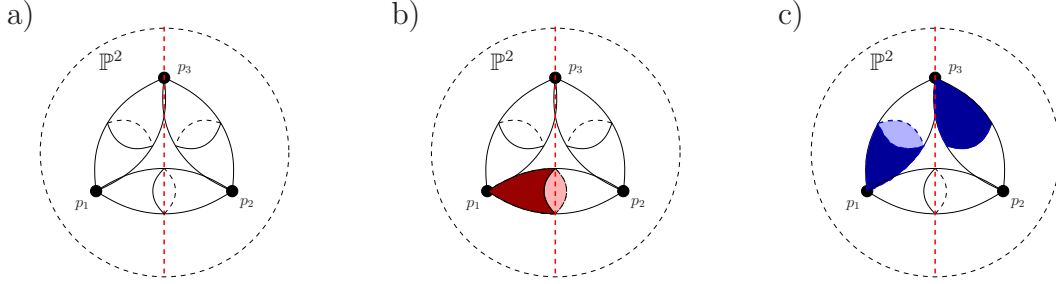


**Figure 1:** a) The orientifold is chosen to act on  $\mathbb{P}^2$  such that the  $\hat{\mathbb{T}}$  fixed points  $p_1$  and  $p_2$  are identified, while  $p_3$  is mapped to itself. The sketched (football-shaped) spheres correspond to the lines  $l_{ij}$ . b) The line  $l_{12}$  can be mapped to from either a disk or a cross-cap. c) The line  $l_{13}$  corresponds in the quotient either to a 2-sphere by gluing disks of different color or to a Klein handle by gluing two disks of the same color.

## 2.2 Orientifolded localization

In order to calculate the remaining contributions to  $\mathcal{G}^{(x)}$  via localization, one would like to replace  $\overline{\mathcal{M}}_d^\Sigma$  by something like the moduli space  $\overline{\mathcal{M}}_d^\Sigma$  of stable maps  $f : \Sigma \rightarrow C$  from curves  $\Sigma$  of Euler characteristic  $\chi$  (with boundaries and cross-caps) into  $\mathbb{P}^2$  with image  $d$  in the relative homology group  $d \in H_2(\mathbb{P}^2, L; \mathbb{Z})$ .

The proper mathematical definitions related to  $\overline{\mathcal{M}}_d^\Sigma$  have so far not been given, except when  $\Sigma$  is the disk [20]. Nevertheless, and following [3], we can give a computational scheme that allows the evaluation of a putative virtual fundamental class of  $\overline{\mathcal{M}}_d^\Sigma$ , after localization. The main reason for this simplification is that after implementing the tadpole cancellation condition of [3], we effectively only need to count maps that send any boundary to a non-trivial one-cycle on  $L$ , and that do not contract any cross-caps. As a result, we have to deal only with moduli spaces of  $n$ -pointed genus  $g$  curves, as without orientifold projection, and also avoid potentially dangerous regions in moduli space where a node lies right on top of the orientifold-plane.

To begin, we choose the involution  $I$  such that it is maximally compatible with the covering space action  $\hat{\mathbb{T}}$ . This means that the projection leaves a subtorus  $\mathbb{T} \cong \mathbb{C}^* \subset \hat{\mathbb{T}}$  intact. Such an  $I$  identifies two of the three covering space fixed-points  $p_i$  and as well two of the fixed-lines  $l_{ij}$ . We arrange it such that  $p_1$  is identified with  $p_2$ . The corresponding action  $I$  is sketched in figure 1a. We infer that  $l_{12}$  is mapped to itself and can receive a disk or a cross-cap, as sketched in figure 1b. Note that one can glue

two of these disks or two cross-caps to obtain a 2-sphere or a Klein handle, respectively. The line  $l_{13}$  can correspond to either a 2-sphere or a Klein handle. How that Klein handle occurs is sketched in figure 1c. In detail, one half of the line can be thought to correspond to the line  $l_{13}$  while the other half comes from the mirror line  $l_{23}$ .

As in the case without orientifold projection, we can pull back the  $\mathbb{T}$  action to an action on  $\overline{\mathcal{M}}_d^\Sigma$ . We will denote the  $\mathbb{T}$  invariant subspace as  ${}^{\mathbb{T}}\overline{\mathcal{M}}_d^\Sigma$ . Due to our restriction to homologically non-trivial boundaries, we have that  $\Sigma$  can only be the union of  $n$ -pointed irreducible genus  $g$  curves mapping under  $f$  to one of the two non-invariant torus fixed points  $p_1, p_2$ , and joined together by either 2-spheres or Klein handles. Furthermore, irreducible disk or cross-cap components can be attached to a contracted component. As before, it follows that each map  $f$  can be represented combinatorially as a connected graph  $\Gamma$ , with a bit of additional decoration.

The contracted component curves correspond again to vertices decorated with the genus of each component, as well as by the point it maps to in target space. As before, the 2-spheres joining the contracted components are mapped to edges connecting the corresponding vertices. As a novelty, the Klein handles joining contracted components are identified with Klein edges, which we may draw as an edge with a cross on top. Note that a Klein edge can be attached to a single vertex, *i.e.*, it may form a loop (in distinction to an ordinary edge). We will refer to these Klein edges also as external Klein edges, while the Klein edges connecting two distinct vertices will be referred to as internal Klein edges. The disks and the cross-caps map to half-edges (also known as legs), or cross-edges attached to the vertices corresponding to the contracted component to which the disk or cross-cap are attached to, respectively. We will draw these simply as half-edges or half-edges with an arrow, attached to vertices (with  $i(v) = 1$  or  $2$  decoration). Note that there is a non-trivial restriction on graphs with Klein edges. Namely, since a Klein edge represents a handle (with orientation reversal), a proper graph should not split into disconnected components after removal of a Klein edge.

As in the unorientifolded theory, each vertex can be associated to an ordinary moduli space  $\overline{\mathcal{M}}_{g_v, val(v)}$ , such that the full graph corresponds to the moduli space

$$\overline{\mathcal{M}}_\Gamma = \prod_v \overline{\mathcal{M}}_{g_v, val(v)} . \quad (2.8)$$

Again, there is a morphism  $\gamma_\Gamma : \overline{\mathcal{M}}_\Gamma \rightarrow M_d^\Gamma \subset {}^{\mathbb{T}}\overline{\mathcal{M}}_d^\Sigma$ , which becomes an isomorphism

if we quotient by  $\mathbb{A}_\Gamma$ , the automorphism group of  $\overline{\mathcal{M}}_\Gamma$ . Thus,

$$\mathbb{T}\overline{\mathcal{M}}_d^\Sigma \cong \bigcup_{\Gamma} (\overline{\mathcal{M}}_\Gamma / \mathbb{A}_\Gamma) . \quad (2.9)$$

However, one has to be extra careful with  $\mathbb{A}_\Gamma$ . In order to illustrate why, let us slightly change our point of view.

To each curve  $\Sigma$  we can associate a corresponding covering curve  $\hat{\Sigma}$  with  $\Sigma = \hat{\Sigma}/\sigma$ . The covering space curve  $\hat{\Sigma}$  has genus  $\hat{g} = \chi + 1$ . Moreover each map  $f$  can be lifted to a covering space map  $\hat{f}$  which is equivariant:

$$\hat{f} = I \circ \hat{f} \circ \sigma^{-1} . \quad (2.10)$$

That is, the following diagram commutes:

$$\begin{array}{ccc} \hat{\Sigma} & \xrightarrow{\hat{f}} & X \\ \sigma \downarrow & & \downarrow I \\ \hat{\Sigma} & \xrightarrow{\hat{f}} & X \end{array} \quad (2.11)$$

Thus,  $\overline{\mathcal{M}}_d^\Sigma$  can as well be defined as the fixed locus of the moduli space  $\overline{\mathcal{M}}_d^{\hat{\Sigma}}$  of the corresponding doubled curve, *i.e.*,  $\overline{\mathcal{M}}_d^\Sigma = \omega^* \overline{\mathcal{M}}_d^{\hat{\Sigma}}$ , with  $\omega^*$  the map obtained by conjugating with  $I$  and  $\sigma$ , as in (2.10). In particular,

$$\mathbb{T}\overline{\mathcal{M}}_d^\Sigma = \omega^* \hat{\mathbb{T}}\overline{\mathcal{M}}_d^{\hat{\Sigma}} . \quad (2.12)$$

Recall that to each  $\hat{f} \in \hat{\mathbb{T}}\overline{\mathcal{M}}_d^{\hat{\Sigma}}$  and  $f \in \mathbb{T}\overline{\mathcal{M}}_d^\Sigma$  we have associated a corresponding graph  $\hat{\Gamma}$ , or  $\Gamma$ , respectively. In thinking about these various identifications, and their automorphism groups, one's first naive expectation is that

$$\Gamma = \hat{\Gamma} / \omega^* , \quad (2.13)$$

holds, with

$$|\text{Aut}(\Gamma)| = |\text{Aut}(\hat{\Gamma})^*| , \quad (2.14)$$

where  $\text{Aut}(\hat{\Gamma})^*$  is the subgroup of  $\text{Aut}(\hat{\Gamma})$  that commutes with  $\omega^*$ . Note that  $\omega^*$  acting on  $\Gamma$  leaves no vertices fixed, due to our restriction to non-trivial boundaries and cross-caps.

To see that the relation is more subtle than described in (2.13) and (2.14), note first that the inverse of relation (2.13) is always true. Namely, to a given graph  $\Gamma$

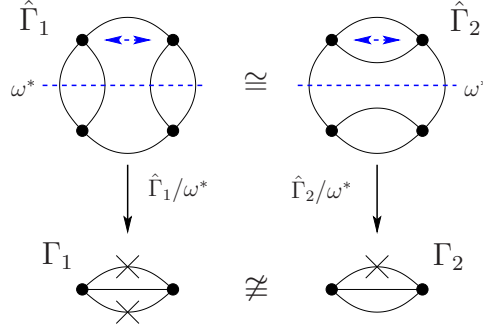


**Figure 2:** The two graphs  $\Gamma_1 \not\cong \Gamma_2$  can potentially contribute to  $\tilde{n}_6^{(2,0)_k}$ . However, we have that  $\hat{\Gamma}_1 \cong \hat{\Gamma}_2$ , with  $\Gamma_1 = \hat{\Gamma}_1/\omega^*$  and  $\Gamma_2 = \hat{\Gamma}_2/\omega^*$ , hence only one should contribute to  $\tilde{n}_6^{(2,0)_k}$ .

we can associate a corresponding covering space graph  $\hat{\Gamma}$  via the following “doubling” procedure: For each vertex  $v$  draw a corresponding mirror vertex  $v'$  with same  $v(g)$  but mirror  $i(v)$  decoration and for each edge draw a corresponding mirror edge. Then, for each disk and cross-cap connected to a vertex, draw an edge connecting the vertex with its mirror. Further, for each external Klein edge draw two edges connecting the vertex and its mirror, while for each internal Klein edge connecting the vertices  $v_1$  and  $v_2$  draw an edge connecting  $v_1$  to  $v'_2$  and one connecting  $v_2$  to  $v'_1$ , where  $v'_i$  are the mirror vertices.

However, while this doubling procedure gives a well-defined map  $\Gamma \mapsto \hat{\Gamma}$ , there is generally no good inverse, *i.e.*, relation (2.13) does not hold in general. For example, consider the graphs  $\hat{\Gamma}_1$  and  $\hat{\Gamma}_2$  shown in figure 2. Both belong to the same equivalence class  $[\hat{\Gamma}]$ , *i.e.*, there exists an isomorphism  $a : \hat{\Gamma}_1 \rightarrow \hat{\Gamma}_2$ , equivariant with respect to  $\omega^*$ . However, the corresponding quotient graphs under  $\omega^*$  are not isomorphic. This is because in general the quotient graph  $[\hat{\Gamma}]/\omega^*$  depends on the choice of representative of  $[\hat{\Gamma}]$ , *i.e.*, we have that

$$[\hat{\Gamma}]/\omega^* = \bigcup_i [\Gamma_i], \quad (2.15)$$

where  $[\Gamma_i]$  are equivalence classes of non-isomorphic quotient graphs  $\Gamma_i$ . Nevertheless, the equivariance condition for  $\hat{f}$  implies that we should include only one graph  $\Gamma \in \{\Gamma_i\}$ , since  $\hat{f}$  should descend to a unique  $f$ .

Hence, the relations  $M_d^\Gamma = \omega^* M_d^{\hat{\Gamma}} \subset \mathbb{T} \overline{\mathcal{M}}_d^\Sigma$ , and (2.13), should be understood in the sense that they may include a choice of representative of  $[\hat{\Gamma}]$ . However, note that

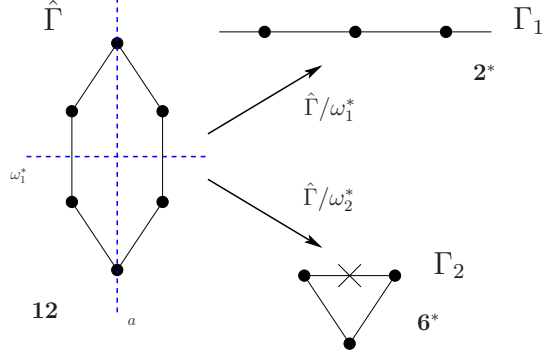


**Figure 3:** The cyclic graph  $\hat{\Gamma} = C_6$  with two differently acting involutions  $\omega_i^*$ . The involution  $\omega_1^*$  yields a quotient graph  $\Gamma_1$  with two half-edges contributing to  $\tilde{n}_6^{(0,2)}$ , while the involution  $\omega_2^* = (a\omega_1^*)$  results in a graph  $\Gamma_2$  with a Klein edge contributing to  $\tilde{n}_6^{(1,0)k}$ . The bold-face number is  $|\text{Aut}(\hat{\Gamma})|$ , while the bold-face numbers with star are the orders of the subgroups of  $\text{Aut}(\hat{\Gamma})$  that commute with  $\omega_i^*$ .

independent of a choice of representative, we have

$$\overline{\mathcal{M}}_{\Gamma} = \omega^* \overline{\mathcal{M}}_{\hat{\Gamma}} = \sqrt{\overline{\mathcal{M}}_{\hat{\Gamma}}} . \quad (2.16)$$

The lesson we learn is the following. In order to avoid multiple countings we have to include in (2.9) only one representative of  $\hat{\Gamma}/\omega^*$ . In practice, this means that we have to perform an extended isomorphism test on the set of graphs  $\{\Gamma\}$ , *i.e.*, two graphs need to be considered as identical if they are firstly isomorphic after replacement of Klein edges with normal edges or if they secondly lift to the same covering graph.

Let us now take a closer look at the relation (2.14). As an illustrative example, consider the graph  $\hat{\Gamma}$  with the two differently acting projections  $\omega_i^*$  sketched in figure 3. We see that  $\omega_1^*$  satisfies condition (2.14), while  $\omega_2^*$  not. This raises the question whether  $\mathbb{A}_{\Gamma}$  involves  $\text{Aut}(\Gamma)$  or  $\text{Aut}(\hat{\Gamma})^*$ . Again, the equivariance condition implies that  $\text{Aut}(\hat{\Gamma})^*$  is the correct choice. Hence,

$$\mathbb{A}_{\Gamma} = \text{Aut}(\hat{\Gamma})^* \times \left( \prod_c \mathbb{Z}_{d_c} \prod_e \mathbb{Z}_{d_e} \prod_k \mathbb{Z}_{d_k} \prod_h \mathbb{Z}_{d_h} \right) , \quad (2.17)$$

where  $k$  runs over the set of Klein edges,  $h$  the set of half-edges and  $c$  the set of cross-caps, if present.

Finally, incorporating the tadpole condition of [3], which tells us that graphs involving disks with even degree cancel against graphs with cross-caps, we deduce that

the set  $\{\Gamma\}$  contributing to  $\tilde{n}_d^{(g,h)}$  and  $\tilde{n}_d^{(g,h)_k}$  includes all non-isomorphic and extended-non-isomorphic graphs  $\Gamma$  which fulfill the following criteria:

- $d_h$  is odd for all half-edges.
- $2 \sum_e d_e + 2 \sum_k d_k + \sum_h d_h = d$ .
- $1 - 2|v| + 2|e| + 2|k| + |h| + 2 \sum_v g_v = g$ , where  $|k|$  is the number of Klein edges and  $|h|$  the number of half-edges.
- Edges connect only vertices with  $i(e) \neq j(e)$ .
- Half-edges are only attached to vertices with  $i(v) = 1$  or  $2$ .
- Klein edges only connect vertices with  $i(k) = j(k)$  or with  $i(k) = 1$  or  $2$  and  $j(k) = 3$  or vice-versa.

Then, with  $\Gamma = \hat{\Gamma}/\omega^*$  we obtain from (2.4):

$$\tilde{n}_d^\Sigma = (-1)^{3g-3+h} \sum_\Gamma \frac{(-1)^{|k|}}{|\mathbb{A}_\Gamma|} \int_{\mathcal{M}_\Gamma} \sqrt{\frac{\mathbf{e}(i^* \mathcal{E}_d)}{\mathbf{e}(\mathcal{N}_{\hat{\Gamma}}^{vir})}}, \quad (2.18)$$

where the sum runs over the set  $\{\Gamma\}$  specified above. Note that our discussion does not a priori fix the overall sign nor the sign of each individual graph. However, most of the sign factors in (2.18) can actually be borrowed from the tree-level discussion in [20]. The remaining signs were determined in [3] based on computations on compact models, comparison with the B-model, and integrality of Gopakumar-Vafa invariants. The existence of the sign  $(-1)^k$  can also be inferred from the requirement that the contribution of a given class of equivariant graphs should be independent of the chosen quotient representative, see discussion around eq. (2.15).

The contribution of vertices, edges and Klein edges of the quotient space graph  $\Gamma$  to the integrand of (2.18) is as before accounted for by (2.5) and (2.6), and supplemented by the following modifications. For each half-edge ending on a vertex  $v$ , add a flag  $(v, h)$  to the set of flags of  $v$ . Define  $i(h)$  as the image point  $p_i$  to which  $v$  maps in target space and  $j(h)$  the image point  $p_j$  of the corresponding mirror-vertex in the covering graph. We also multiply the integrand by the following factor accounting for



the half-edges. (This is essentially just a squareroot of an ordinary edge contribution.)

$$\begin{aligned}
D(\Gamma) = & \prod_h \frac{(-1)^{\frac{d_h-1}{2}} d_h^{d_h}}{(d_h!) (\lambda_{i(h)} - \lambda_{j(h)})^{d_h}} \prod_{\substack{k \neq i(h), j(h) \\ a=0}}^{\frac{d_h-1}{2}} \frac{1}{\frac{a}{d_h} \lambda_{i(h)} + \frac{d_h-a}{d_h} \lambda_{j(h)} - \lambda_k} \\
& \times \prod_h^{\frac{3d_h-1}{2}} \left[ \Lambda_{i(h)} + \frac{m}{d_h} (\lambda_{i(h)} - \lambda_{j(h)}) \right].
\end{aligned} \tag{2.19}$$

The Klein edges are treated like usual edges, however with  $i(k)$  and  $j(k)$  defined as  $i(v)$  and  $j(v)$  of the corresponding covering graph edge. At the very end, we need to identify in the integrand  $\lambda_1 = -\lambda_2$ . Then we cancel any common factors between numerator and denominator from each summand. These could cause ill-defined “ $\frac{0}{0}$ ”-type expressions when we set  $\lambda_3 = 0$  in the final expression for  $\tilde{n}_d^\Sigma$ .

We have developed a full computer implementation of the above prescription and used it to calculate the open and unoriented Gromov-Witten invariants up to  $\chi = 9$  for various degrees. We will not list the complete data, but rather just give the real Gopakumar-Vafa invariants which we were able to verify with our data, see appendix A. Some of the Gromov-Witten invariants that we obtained can be inferred from the large-volume expansions given in section 4.2. These amplitudes were computed by using our localization data to fix the holomorphic ambiguities of the B-model. This will be explained in detail in section 4.

### 3 The real topological vertex

The localization computations of the previous section quickly become rather complicated with increasing genus and degree. There are two sources of complexity. First, one has to generate the decorated graphs and correctly determine their automorphism groups. As we have seen, this can be tricky especially in the real case. Second, one has to evaluate the graphs, and in particular to compute the Hodge integrals. The best available general algorithm for this still is Faber’s. On the other hand, note that the computation of the Hodge integral is a local problem, attached to the fixed points of the torus action. Some years ago, it has been realized that there is in fact a closed formula that resums the requisite Hodge integrals to all orders in the genus expansion, and that incidentally also solves the first-mentioned graph combinatorial problem in a very efficient way. This is the topological vertex [10].

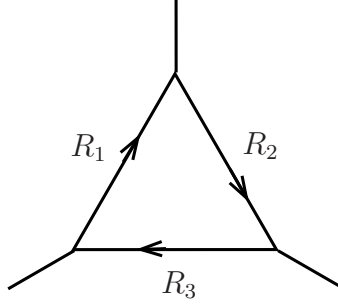


**Figure 4:** Trivalent diagram representing local  $\mathbb{P}^2$  for the purposes of evaluating the topological vertex.

### 3.1 Topological vertex for local $\mathbb{P}^2$

Instead of setting up the full formalism of [10], we give here an elementary account of the topological vertex at work on local  $\mathbb{P}^2$ . This will be sufficient to write down the formulas that compute the amplitudes also in the real case.

The toric diagram representing local  $\mathbb{P}^2$  as a  $T^2 \times \mathbb{R}$  fibration over a three-dimensional base is shown in figure 4. According to [21, 22], the total closed topological string partition function of local  $\mathbb{P}^2$  is given by

$$Z = \sum_{R_1, R_2, R_3} (-1)^{\sum l(R_i)} q^{-\sum \kappa_{R_i}} e^{-t \sum l(R_i)} C_{0R_3^t R_1} C_{0R_2^t R_3} C_{0R_1^t R_2} . \quad (3.1)$$

In this sum, the  $R_i$  run over all Young diagrams (representations of  $U(\infty)$ ),  $l(R_i)$  is the number of boxes in  $R_i$ , and  $\kappa(R_i)$  is related to the second Casimir of the corresponding representation. These initial factors come from the need to adjust the framing on the internal legs between the vertices. But the central ingredient of (3.1) is the topological vertex itself. The full three-legged vertex (in the canonical framing) is given by

$$C_{R_1 R_2 R_3} = q^{\kappa_{R_2}/2 + \kappa_{R_3}/2} \sum_{Q, Q_1, Q_3} N_{QQ_1}^{R_1} N_{QQ_3}^{R_3} \frac{W_{R_2^t Q_1} W_{R_2 Q_3^t}}{W_{R_2 0}} , \quad (3.2)$$

where the  $N_{QQ_1}^{R_1}$  are the  $U(\infty)$  tensor product coefficients, and  $W_{R_1 R_2} = W_{R_1 R_2}(q)$  is a certain rational function of  $q$  that arises by taking a specific limit (in level and rank) of the Chern-Simons invariant of the Hopf link in  $S^3$  decorated with  $R_1$  and  $R_2$ . When one of the representations on the vertex is trivial, we have the more compact expression

$$C_{0R_1 R_2} = q^{\kappa_{R_2}/2} W_{R_1 R_2} . \quad (3.3)$$

In all these formulas, we have adopted the standard topological vertex notation in which  $t$  still denotes the Kähler parameter of  $\mathbb{P}^2$ , but  $q = e^\lambda$  is the exponentiated string coupling. We make full contact with the previous notation by relating the free energy in those variables to the Gopakumar-Vafa invariants (cf. (1.6))

$$\mathcal{F} = \log Z = \sum_{d,g,k} N_d^{(g)} \frac{1}{k} (q^{k/2} - q^{-k/2})^{2g-2} e^{-tkd} . \quad (3.4)$$

### 3.2 Taking a squareroot

We are now in a position to present the formulas that express the real topological string amplitudes of local  $\mathbb{P}^2$  in terms of the (real) topological vertex. The basic idea is the following. The topological vertex can be viewed as an all-genus resummation of the local contribution at each vertex on the toric diagram to the localization formulas for the topological string amplitude (see, *e.g.*, [23]). Going from the ordinary topological string to the real topological string amounts in the localization formalism to first restrict to the graphs fixed under the target space involution, and then take a squareroot of each individual contribution. The only conceptual difficulty is to understand which sign of the squareroot to take.

Taking these observations together, all we have to do to obtain a real vertex formalism is to identify the action of the target space involution on the toric diagram of figure 4 and on formulas (3.1) and (3.2), and then to take an appropriate squareroot. It is in fact not hard to see that the action on the representations is  $R_1 \mapsto R_2$  and  $R_3 \mapsto R_3$ . Using the symmetry of the topological vertex

$$C_{R_1 R_2 R_3} = q^{\sum \kappa_{R_i}/2} C_{R_1^t R_3^t R_2^t} , \quad (3.5)$$

we see that for the fixed configurations,  $R_1 = R_2$ , the summand in (3.1) is of the form.

$$(-1)^{2l(R_1)+l(R_3)} q^{-5\kappa_{R_1}/2 - \kappa_{R_3}/2} e^{-t(2l(R_1)+l(R_3))} (C_{0R_3^t R_1})^2 C_{0R_1^t R_1} . \quad (3.6)$$

This is a perfect square except for the final term, which arises at the vertex fixed under the involution. Such a term will arise in general toric Calabi-Yaus with involution that leaves some vertices fixed, but permutes two of the legs ending on it. In that case, we will generally require a “real topological vertex” that might be obtained by taking an appropriate squareroot of the expression (3.2) for the topological vertex with  $R_3 = R_1^t$ , and  $R_2 = R_2^t$ . Indeed, we see that with this external data, and restriction of the sum

to  $Q_3 = Q_1^t$ , the vertex is itself almost a sum of squares,

$$(N_{QQ_1}^{R_1})^2 \frac{(W_{R_2^t Q_1})^2}{W_{R_2 0}}, \quad (3.7)$$

except for the  $W_{R_2 0}$  in the denominator. We do not know at present how to take a squareroot of that last term. But luckily, for our application to local  $\mathbb{P}^2$ , we only need the two-legged vertex, and the real vertex only with trivial representation  $R_2 = 0$  on the fixed leg. Based on the above observations, we propose the following expression for that real vertex amplitude

$$C_{R_1 0}^{\text{real}} = q^{-\kappa_{R_1}/4} \sum_{Q, Q_1} N_{QQ_1}^{R_1} W_{Q_1 0}. \quad (3.8)$$

Returning to the formula for local  $\mathbb{P}^2$ , we obtain for the partition function of the real topological string

$$Z^{\text{real}} = \sum_{R_1, R_3} (-1)^{l(R_1)} (-1)^{p(R_3)} e^{-t(l(R_1)+l(R_3)/2)} q^{-5\kappa_{R_1}/4 - \kappa_{R_3}/4} C_{R_1 0}^{\text{real}} C_{0R_3^t R_1}, \quad (3.9)$$

where  $(-1)^{p(R_3)} = \pm 1$  is an a priori undetermined sign. Note that for symmetry reasons, this sign can only depend on  $R_3$ , as we have indicated. Some experimentation shows that its correct value is determined by the *number of boxes in even columns*. In other words, if  $R_3^t$  consists of rows of length  $l_1, \dots, l_r$ , then

$$(-1)^{p(R_3)} = (-1)^{\sum_i l_{2i}}. \quad (3.10)$$

We are not aware that such a sign associated with 2d partitions has appeared before, nor does there seem to be any representation theoretic meaning. This would be worthy of clarification.

In any event, we can now make contact with the other expressions for the amplitudes of real local  $\mathbb{P}^2$ . The real analogue of (3.4), see also (1.11), is

$$\log Z^{\text{real}} = \frac{1}{2} \mathcal{F} + \sum_{\substack{d \equiv \chi \pmod{2} \\ k \text{ odd}}} N_d^{t(\chi)} \frac{1}{k} (q^{k/2} - q^{-k/2})^\chi e^{-tkd/2} \epsilon^\chi. \quad (3.11)$$

These formulas reproduce the localization results of the previous section, wherever the available data has allowed comparison, and also agree with the developments of the B-model to which we turn presently.

To close this section, we point out that we have merely scratched the surface of the real topological vertex. Starting with the derivation, but including its properties, applications, and connections with other theories, one can ask for a real counterpart of essentially everything that is known about the ordinary topological vertex. The central question in this endeavour is whether the signs can be understood in a uniform way. We have to leave this for the future.

## 4 The B-model

We now turn to a computation of the real topological string amplitudes using the mirror B-model. Here again, most of the technology is already in place in the literature, so we will be rather brief, and just restate the formulas in our chosen normalization. The main aim is to push the holomorphic anomaly technique to higher order in perturbation theory. Besides reproducing the A-model results from section 2 and the results from the real topological vertex from section 3, the main payoff will be a new gap structure in the expansion of the real topological string amplitudes at the conifold.

In order to set the stage, let us briefly recall some basic facts. While we introduced the A-model topological string free energies  $\mathcal{F}(t)$ ,  $\mathcal{K}(t)$  and  $\mathcal{G}(t)$  in a rather geometric way as a count of holomorphic maps from world-sheets with specific topology into a Calabi-Yau manifold with Kähler parameter  $t$ , it is important to note that this interpretation only holds at large volume. Away from this point in moduli space, classical notions of geometry break down and so does the original interpretation of the free energies. On the other hand, the proper definition of the perturbative amplitudes is really in terms of the topologically twisted 2d world-sheet theory, which is well-defined over the entire stringy Kähler moduli space. Here it is where mirror symmetry comes to rescue, since the A-twisted world-sheet theory on  $X$  is equivalent to a B-twisted theory on a mirror Calabi-Yau geometry  $Y$ , with Kähler parameter traded for complex structure, such that the B-model captures the quantum regime of the A-model. In particular, the corresponding B-model amplitudes  $\mathcal{F}(z, \bar{z})$ ,  $\mathcal{K}(z, \bar{z})$  and  $\mathcal{G}(z, \bar{z})$  are now functions over the complex structure moduli space of  $Y$ , which we will denote as  $\mathcal{M}_Y$ .

A key point that allows to efficiently solve for the amplitudes in the B-model is that their anti-holomorphic derivatives over  $\mathcal{M}_Y$  do not vanish [13], as we have indicated in the notation. The so-called holomorphic anomaly equations [13, 14, 3], completely determine the anti-holomorphic dependence of the amplitudes, and reduce the prob-

lem to the fixing of the holomorphic part. Constraints of modular invariance and a priori knowledge about the compactification of the moduli space make this a finite-dimensional problem. Its general solution is still rather elusive, but important progress has been made in recent years. An additional bonus of the B-model is the possibility to analyze the structure of the amplitudes at special points in moduli space other than large volume.

#### 4.1 Solving the (extended) holomorphic anomaly equations

The extended holomorphic anomaly equations of [14, 3], specialized to the local 1-parameter case, are given by

$$\partial_{\bar{z}}\mathcal{F}^{(g,h)} = \frac{1}{2} \sum_{\substack{g_1+g_2=g \\ h_1+h_2=h \\ 2g_i+h_i>1}} C_{\bar{z}}^{zz} \mathcal{F}_z^{(g_1,h_1)} \mathcal{F}_z^{(g_2,h_2)} + \frac{1}{2} C_{\bar{z}}^{zz} \mathcal{F}_{zz}^{(g-1,h)} - \Delta_{\bar{z}}^z \mathcal{F}_z^{(g,h-1)} , \quad (4.1)$$

and

$$\begin{aligned} \partial_{\bar{z}}\mathcal{K}^{(g,h)} = & \sum_{\substack{g_1+g_2=g \\ h_1+h_2=h \\ 2g_2+h_2>1 \\ g_1>0}} C_{\bar{z}}^{zz} \mathcal{K}_z^{(g_1,h_1)} \mathcal{F}_z^{(g_2,h_2)} + \frac{1}{2} \sum_{\substack{g_1+g_2=g \\ h_1+h_2=h \\ g_i>0}} C_{\bar{z}}^{zz} \mathcal{K}_z^{(g_1,h_1)} \mathcal{K}_z^{(g_2,h_2)} \\ & + C_{\bar{z}}^{zz} \mathcal{K}_{zz}^{(g-1,h)} + \frac{1}{2} C_{\bar{z}}^{zz} \mathcal{F}_{zz}^{(g-1,h)} - \Delta_{\bar{z}}^z \mathcal{K}_z^{(g,h-1)} , \end{aligned} \quad (4.2)$$

where  $\mathcal{F}_{z\dots z} = D_z \cdots D_z \mathcal{F}$ , similarly for the  $\mathcal{K}$ , and  $z$  is a local coordinate on the space of complex structures,  $\mathcal{M}_Y$ , of  $Y$ . Further,  $C_{zzz}$  is the usual Yukawa-coupling, *i.e.*, the sphere three-point function, and  $\Delta_{zz}$  is the disk two-point function (with bulk insertions). As usual, indices are raised and lowered via the Kähler metric on  $\mathcal{M}_Y$ . Note that we have here already implemented tadpole cancellation, so we can consistently set the  $\mathcal{R}^{(g,h)}$  to zero.

Equations (4.1) and (4.2) can be solved recursively. Let us for the moment consider the simplified case without open strings, *i.e.*,  $h = 0$ . Then, recursively solved, the equations give an expression for  $\mathcal{F}^{(g,0)}$  and  $\mathcal{K}^{(g,0)}$  in terms of  $\mathcal{F}^{(1,0)}$  and  $\mathcal{K}^{(1,0)}$ . These 1-loop amplitudes have the following holomorphic limits [13, 3]

$$\begin{aligned} \mathcal{F}^{(1,0)} &= \frac{1}{2} \log(\tau) + a_{\mathcal{F}}^{(1,0)} , \\ \mathcal{K}^{(1,0)} &= \frac{1}{2} \log(\tau) + a_{\mathcal{K}}^{(1,0)} , \end{aligned} \quad (4.3)$$

where we defined  $\tau = \partial_t z(t)$  to be the derivative of  $z$  with respect to the preferred flat coordinate  $t$  at the large volume point of  $\mathcal{M}_Y$ . The 1-loop holomorphic ambiguities occurring in (4.3) are for local  $\mathbb{P}^2$  given by

$$\begin{aligned} a_{\mathcal{F}}^{(1,0)} &= -\frac{1}{2} \log(z) - \frac{1}{12} \log(-z) - \frac{1}{12} \log(1 - 27z) , \\ a_{\mathcal{K}}^{(1,0)} &= -\frac{1}{2} \log(z) - \frac{1}{8} \log(1 - 27z) . \end{aligned} \quad (4.4)$$

To proceed, we define the non-holomorphic objects (propagators in Feynman diagram language)  $S^{zz}$  and  $K^{zz}$  as

$$\begin{aligned} S^{zz} &= 2 \frac{\mathcal{F}_z^{(1,0)}}{C_{zzz}} , \\ K^{zz} &= 2 \frac{\mathcal{K}_z^{(1,0)}}{C_{zzz}} , \end{aligned} \quad (4.5)$$

where the Yukawa coupling  $C_{zzz} = \mathcal{F}_{zzz}^{(0,0)}$  reads for local  $\mathbb{P}^2$

$$C_{zzz} = -\frac{1}{3} \frac{1}{z^3(1 - 27z)} . \quad (4.6)$$

Comparing with (4.3), we see that  $K^{zz}$  and  $S^{zz}$  differ only by a holomorphic function

$$K^{zz} = S^{zz} + 2 \frac{\partial_z a_{\mathcal{K}\mathcal{F}}}{C_{zzz}} , \quad (4.7)$$

with

$$a_{\mathcal{K}\mathcal{F}} = a_{\mathcal{K}}^{(1,0)} - a_{\mathcal{F}}^{(1,0)} . \quad (4.8)$$

Hence, we can express both  $\mathcal{F}_z^{(1,0)}$  and  $\mathcal{K}_z^{(1,0)}$  in terms of the single non-holomorphic propagator  $S^{zz}$ , up to holomorphic terms. Furthermore, (using the special geometry relation) it is easy to deduce that one can re-express the covariant derivative of  $S^{zz}$  in terms of  $S^{zz}$ , *i.e.*,

$$D_z S^{zz} = -C_{zzz} (S^{zz})^2 + (a_{DS})_z^{zz} . \quad (4.9)$$

and that a similar condition holds for the connection coefficient  $\Gamma_{zz}^z$ ,

$$\Gamma_{zz}^z = -C_{zzz} S^{zz} + (a_{\Gamma})_{zz}^z . \quad (4.10)$$

Here,  $a_{DS}$  and  $a_{\Gamma}$  are global holomorphic functions. For local  $\mathbb{P}^2$ , and our definition of the propagator (4.5), we have

$$a_{\Gamma} = 2 \partial_z a_{\mathcal{F}}^{(1,0)} = -\frac{7 - 216z}{6z(1 - 27z)} , \quad (4.11)$$

$$a_{DS} = -\frac{z}{12(1 - 27z)} . \quad (4.12)$$

Thus, we conclude that all  $\mathcal{F}^{(g,0)}$  and  $\mathcal{K}^{(g,0)}$  can be expressed as polynomials in the single propagator  $S^{zz}$ , with coefficients given by holomorphic functions in  $z$ . This idea originated in [24], to which we refer for more details about the  $\mathcal{F}^{(g,0)}$  case.

Let us now include the open string sector. With assumptions detailed in [14], the only new ingredient that enters the recursive solution is the disk amplitude with two bulk insertions. In the holomorphic limit, this is given by [14]

$$\Delta_{zz} = \mathcal{F}_{zz}^{(0,1)} = \partial_z \partial_z \mathcal{T}, \quad (4.13)$$

where  $\mathcal{T}$  is the domain-wall tension. As for the closed string case, we can define a non-holomorphic object (terminator in Feynman diagram language)

$$\Delta^z = -\frac{\mathcal{F}_{zz}^{(0,1)}}{C_{zzz}}, \quad (4.14)$$

which for local  $\mathbb{P}^2$  satisfies

$$D_z \Delta^z = \frac{3}{4} \sqrt{z}. \quad (4.15)$$

As a consequence, the amplitudes  $\mathcal{F}^{(g,h)}$  and  $\mathcal{K}^{(g,h)}$  can be expressed in terms of the two non-holomorphic objects  $S^{zz}$  and  $\Delta^z$ , with holomorphic coefficients. A detailed discussion of the (oriented)  $\mathcal{F}^{(g,h)}$  case can be found in [25, 26]. Then, using the relations [13, 14]

$$C_{\bar{z}}^{zz} = \partial_{\bar{z}} S^{zz}, \quad \Delta_{\bar{z}}^z = \partial_{\bar{z}} \Delta^z, \quad (4.16)$$

one can re-express the above extended holomorphic anomaly equations as

$$\begin{aligned} \partial_{S^{zz}} \mathcal{F}^{(g,h)} &= \frac{1}{2} \sum \mathcal{F}_z^{(g_1, h_1)} \mathcal{F}_z^{(g_2, h_2)} + \frac{1}{2} \mathcal{F}_{zz}^{(g-1, h)}, \\ \partial_{\Delta^z} \mathcal{F}^{(g,h)} &= -\mathcal{F}_z^{(g, h-1)}, \end{aligned} \quad (4.17)$$

and

$$\begin{aligned} \partial_{S^{zz}} \mathcal{K}^{(g,h)} &= \sum \mathcal{K}_z^{(g_1, h_1)} \mathcal{F}_z^{(g_2, h_2)} + \frac{1}{2} \sum \mathcal{K}_z^{(g_1, h_1)} \mathcal{K}_z^{(g_2, h_2)} + \mathcal{K}_{zz}^{(g-1, h)} + \frac{1}{2} \mathcal{F}_{zz}^{(g-1, h)}, \\ \partial_{\Delta^z} \mathcal{K}^{(g,h)} &= -\mathcal{K}_z^{(g, h-1)}, \end{aligned} \quad (4.18)$$

These equations can be easily solved by direct integration, up to the holomorphic ambiguities to which we will return momentarily.

Before that, recall that in (1.1) we have identified the total topological string amplitude  $\mathcal{G}^{(x)}$  as a combination of  $\mathcal{F}$ 's and  $\mathcal{K}$ 's (see (1.3), with  $\mathcal{R}^{(g,h)} \equiv 0$ ). It is clear that one can write down a combined holomorphic anomaly equation directly for the



total amplitude  $\mathcal{G}^{(\chi)}$ , which is in fact somewhat simpler [3] (as already stressed in the introduction, we are working here with a different normalization of  $\mathcal{G}^{(\chi)}$ , as a result the combined anomaly equation we are using differs slightly from the one presented in [3])

$$\partial_{\bar{z}}\mathcal{G}^{(\chi)} = \frac{1}{2} \sum_{\substack{\chi_1+\chi_2=\chi-2 \\ \chi_i \geq 0}} C_{\bar{z}}^{zz} \mathcal{G}_z^{(\chi)} \mathcal{G}_z^{(\chi)} + C_{\bar{z}}^{zz} \mathcal{G}_{zz}^{(\chi-2)} - \Delta_{\bar{z}}^z \mathcal{G}_z^{(\chi-1)} . \quad (4.19)$$

It is obvious that just as the individual amplitudes  $\mathcal{F}$  and  $\mathcal{K}$ ,  $\mathcal{G}^{(\chi)}$  can be written as a polynomial in the non-holomorphic propagator  $S^{zz}$  and terminator  $\Delta^z$ , with holomorphic coefficients. Thus, we can re-express (4.19) as

$$\begin{aligned} \partial_{S^{zz}}\mathcal{G}^{(\chi)} &= \frac{1}{2} \sum \mathcal{G}_z^{(\chi)} \mathcal{G}_z^{(\chi)} + \mathcal{G}_{zz}^{(\chi-2)} , \\ \partial_{\Delta^z}\mathcal{G}^{(\chi)} &= -\mathcal{G}_z^{(\chi-1)} , \end{aligned} \quad (4.20)$$

which again can be simply solved by integration, yielding a polynomial in  $S^{zz}$  and  $\Delta^z$  with holomorphic functions in  $z$  as coefficients.

## 4.2 Fixing the holomorphic ambiguities

In order to evaluate the polynomials in  $S^{zz}$  and  $\Delta^z$  that we have obtained by integrating the holomorphic anomaly equation, *i.e.*, to obtain explicit expansions of  $\mathcal{F}$ ,  $\mathcal{K}$  and  $\mathcal{G}$ , we have to specify the coordinate  $z$ . That is, we have to choose a point in moduli-space around which to expand these amplitudes. Furthermore, the holomorphic ambiguities of these amplitudes, which we will denote as  $a_{\mathcal{F}/\mathcal{K}}^{(g,h)}$  and  $a_{\mathcal{G}}^{(\chi)}$ , have to be fixed.

The natural point of interest in moduli space is the large-volume point with flat coordinate  $t$  corresponding to the Kähler parameter of  $\mathbb{P}^2$ . At this point, we can compare with our results from localization and the real topological vertex to fix the ambiguities  $a_{\mathcal{F}/\mathcal{K}}^{(g,h)}$  and  $a_{\mathcal{G}}^{(\chi)}$ . The mirror map  $z(t)$  and the domain-wall tension  $\mathcal{T}$  that enters into  $\Delta^z(t)$  can be obtained from the (inhomogenous) Picard-Fuchs equation (we have taken the liberty to multiply the inhomogeneous part with an additional factor of  $-i(2\pi)^2$  in comparison with [3])

$$(\theta^3 - 3z\theta(3\theta + 1)(3\theta + 2)) \mathcal{T} = -\frac{1}{4}\sqrt{z} , \quad (4.21)$$

with  $\theta = z\partial_z$ . The solutions of the homogenous equation near  $z = 0$  yield the well-known closed string periods (leading to the mirror map  $z(t)$ ), while the solution of the

inhomogeneous equation gives the domain-wall tension interpolating between the two open string vacua (recall that we have a discrete  $\mathbb{Z}_2$  valued Wilson-line on the brane).

$$\mathcal{T} = 2i \Gamma(3/2)^2 \sum_{n=0}^{\infty} \frac{\Gamma(3n + 3/2)}{\Gamma(n + 3/2)^3} z^{n+1/2} . \quad (4.22)$$

Using the definitions (4.5) and (4.14), we obtain the following large-volume expansions of the  $z(t)$ ,  $S^{zz}(t)$  and  $\Delta^z(t)$

$$\begin{aligned} z(t) &= -q - 6q^2 - 9q^3 - 56q^4 + 300q^5 - 3942q^6 + 48412q^7 - \dots , \\ S^{zz}(t) &= \frac{1}{2}q^2 + 15q^3 + 135q^4 + 785q^5 + \frac{4473}{2}q^6 + 18333q^7 - \dots , \\ -i\Delta^z(t) &= -\frac{3}{2}q^{3/2} - \frac{39}{2}q^{5/2} - \frac{117}{2}q^{7/2} - \frac{765}{2}q^{9/2} + 1881q^{11/2} - \dots , \end{aligned} \quad (4.23)$$

with  $q = e^{2\pi it}$ . Note that

$$S^{zz}(t) = \tau^2 S^{tt}, \quad S^z(t) = \tau \Delta^t . \quad (4.24)$$

where  $\tau = \partial_t z(t)$ . Plugging these expansions into the polynomial expressions for  $\mathcal{F}$  and  $\mathcal{K}$  and comparing with our localization results allows us to fix the holomorphic ambiguities up to a certain order. We here report our observations.

First of all, the holomorphic ambiguities of  $\mathcal{F}^{(0,h)}$ ,  $\mathcal{F}^{(1,h)}$  and  $\mathcal{K}^{(1,h)}$  take a very simple form. More precisely, in our scheme, the ambiguities  $a_{\mathcal{F}}^{(0,h)}$  and  $a_{\mathcal{K}}^{(1,h)}$  all vanish, whereas we find for the ambiguity  $a_{\mathcal{F}}^{(1,h)}$  of  $\mathcal{F}^{(1,h)}$

$$a_{\mathcal{F}}^{(1,h)} = \begin{cases} -\frac{1}{24}z^{1/2} & h = 1 \\ (-1)^h \frac{3^{(h-1)}}{2^{(2h+2)h}} z^{h/2} & h > 1 \end{cases} . \quad (4.25)$$

Secondly, one may note that the open string degenerations alone completely generate all Feynman diagrams for  $\mathcal{F}^{(0,h)}$ ,  $\mathcal{F}^{(1,h)}$ , and  $\mathcal{K}^{(1,h)}$  for all  $h$ . This means that using a flat coordinate  $t$ , we have the following simple expressions for these amplitudes, which can be evaluated even for very large  $h$  most economically:

$$\begin{aligned} \mathcal{F}^{(0,h)} &= \int d\Delta^t \partial_t \mathcal{F}^{(0,h-1)} = \left[ \int d\Delta^t \partial_t \right]^{h-2} \mathcal{F}^{(0,2)}(t) , \\ \mathcal{K}^{(1,h)} &= \int d\Delta^t \partial_t \mathcal{K}^{(1,h-1)} = \left[ \int d\Delta^t \partial_t \right]^h \mathcal{K}^{(1,0)}(t) , \\ \mathcal{F}^{(1,h)} &= \int d\Delta^t \partial_t \mathcal{F}^{(1,h-1)} + a_{\mathcal{F}}^{(1,h)} \\ &= \left[ \int d\Delta^t \partial_t \right]^h \mathcal{F}^{(1,0)}(t) + \sum_{i=1}^h \left[ \int d\Delta^t \partial_t \right]^{(h-i)} a_{\mathcal{F}}^{(1,i)} . \end{aligned} \quad (4.26)$$

For higher genus, things become more involved, and there does not appear to be a simple structure as in (4.25). For illustration, we give here the following oriented open string amplitudes

$$\begin{aligned}
\mathcal{F}^{(2,1)} &= -\frac{7\sqrt{q}}{2880} + \frac{79q^{3/2}}{2880} - \frac{59q^{5/2}}{128} + \frac{2597q^{7/2}}{720} - \frac{205151q^{9/2}}{240} + \frac{31659529q^{11/2}}{640} + \dots, \\
\mathcal{F}^{(2,2)} &= \frac{11q}{3072} + \frac{41q^2}{12288} + \frac{10663q^3}{2560} - \frac{389561q^4}{30720} + \frac{13173223q^5}{3072} - \frac{5413756009q^6}{20480} + \dots, \\
\mathcal{F}^{(2,3)} &= -\frac{87q^{3/2}}{20480} - \frac{3259q^{5/2}}{10240} - \frac{476291q^{7/2}}{20480} - \frac{465417q^{9/2}}{20480} - \frac{348949197q^{11/2}}{20480} + \dots, \\
\mathcal{F}^{(2,4)} &= \frac{407q^2}{81920} + \frac{57861q^3}{32768} + \frac{2103243q^4}{20480} + \frac{15796159q^5}{32768} + \frac{4897896903q^6}{81920} + \dots.
\end{aligned} \tag{4.27}$$

and the following unoriented amplitudes.

$$\begin{aligned}
\mathcal{K}^{(2,0)} &= \frac{5q}{128} + \frac{33q^2}{16} - \frac{10953q^3}{64} + \frac{223495q^4}{32} - \frac{13926207q^5}{64} + \frac{379810917q^6}{64} + \dots, \\
\mathcal{K}^{(2,1)} &= -\frac{9q^{3/2}}{128} - \frac{12723q^{5/2}}{1024} + \frac{270585q^{7/2}}{256} - \frac{13282137q^{9/2}}{256} + \frac{1951535727q^{11/2}}{1024} + \dots, \\
\mathcal{K}^{(2,2)} &= \frac{99q^2}{2048} + \frac{48897q^3}{1024} - \frac{4235175q^4}{1024} + \frac{120073203q^5}{512} - \frac{20153395269q^6}{2048} + \dots, \\
\mathcal{K}^{(2,3)} &= \frac{747q^{5/2}}{4096} - \frac{4921425q^{7/2}}{32768} + \frac{215009073q^{9/2}}{16384} - \frac{27419944149q^{11/2}}{32768} + \dots, \\
\mathcal{K}^{(2,4)} &= -\frac{34749q^3}{32768} + \frac{6909435q^4}{16384} - \frac{1208349657q^5}{32768} + \frac{21269586123q^6}{8192} + \dots.
\end{aligned} \tag{4.28}$$

In all these cases, we have parameterized the holomorphic ambiguities of  $\mathcal{F}^{(g,h)}$  and  $\mathcal{K}^{(g,h)}$  via the function

$$a_{\mathcal{F}/\mathcal{K}}^{(g,h)} = \sum_{i=0}^{n-1} a_i \frac{z^{i+h/2}}{(1-27z)^{2g-2}}, \tag{4.29}$$

where  $a_i$  are rational numbers and

$$n = \begin{cases} 2g - 1 & \text{for } \mathcal{F}^{(g,0)} \\ 3g - 2 & \text{else} \end{cases}. \tag{4.30}$$

We have then compared the coefficients of the  $q$ -expansion in low degree with our localization results in order to determine the coefficients of the holomorphic ambiguity  $a_i$ . Note that the number of coefficients that needs to be fixed is larger for  $h \neq 0$  than in the purely closed string case. This can be traced back to the existence of the tensionless domain wall at the orbifold point and the resulting singularity of the  $\mathcal{F}$  and  $\mathcal{K}$  at this point. On the other hand, it is mildly comforting that the number of unknown coefficients does not grow with  $h$ . (Naively, one might expect  $n \sim 3g + h$  or something similar.) This could suggest that there is additional structure that we have so far not identified. However, hopes of finding a very simple expression as in (4.25) for  $g > 1$  have so far not materialized.

The (individual) amplitudes we have determined so far are only sufficient to obtain  $\mathcal{G}^{(\chi)}$  via relation (1.3) up to  $\chi = 3$  (which has been already achieved in [3]). In order to go beyond we need more information. A prime candidate to look at is the conifold point in moduli space, where it is known that the expansion of the closed string amplitudes  $\mathcal{F}^{(g,0)}$  possesses a “gap”. This structure, whose existence can be understood physically, gives enough information to completely determine these amplitudes for all  $g$  [15, 16, 17]. It is natural to ask whether there is as well some systematics in the expansion of the real topological string amplitudes at the conifold point.

To exhibit the gap, we first need the appropriate flat coordinate. To this end, we solve the Picard-Fuchs equation (4.21) after the variable transformation  $z \rightarrow z' = \frac{1-\Delta}{27}$ , where  $\Delta$  is the discriminant  $\Delta = 1 - 27z$ . Thus,  $\theta \rightarrow \theta' = (\Delta - 1)\partial_\Delta$  and we obtain the known closed string periods at the conifold. In particular, we deduce the local flat coordinate at the conifold  $t_c$  to be,

$$t_c = \sqrt{3}\Delta + \frac{11\Delta^2}{6\sqrt{3}} + \frac{109\Delta^3}{81\sqrt{3}} + \frac{9389\Delta^4}{8748\sqrt{3}} + \frac{88351\Delta^5}{98415\sqrt{3}} + \frac{823187\Delta^6}{1062882\sqrt{3}} + \frac{68584051\Delta^7}{100442349\sqrt{3}} + \dots \quad (4.31)$$

The additional solution  $\mathcal{T}_c$  of the inhomogeneous equation corresponds to the domain-wall tension at the conifold (up to a rational closed string period),

$$\mathcal{T}_c = \frac{\Delta^2}{24\sqrt{3}} + \frac{121\Delta^3}{2592\sqrt{3}} + \frac{3197\Delta^4}{69984\sqrt{3}} + \frac{4372889\Delta^5}{100776960\sqrt{3}} + \frac{222720689\Delta^6}{5441955840\sqrt{3}} + \frac{79384773199\Delta^7}{2057059307520\sqrt{3}} + \dots \quad (4.32)$$

As before, we can then easily infer the expansions of  $z(t_c)$ ,  $S^{zz}(t_c)$ , and  $\Delta^z(t_c)$  at the conifold point. We obtain

$$\begin{aligned} z(t_c) &= \frac{1}{27} - \frac{t_c}{27\sqrt{3}} + \frac{11t_c^2}{1458} - \frac{145t_c^3}{39366\sqrt{3}} + \frac{6733t_c^4}{12754584} - \frac{120127t_c^5}{573956280\sqrt{3}} + \dots, \\ S^{zz}(t_c) &= -\frac{1}{1458} + \frac{4t_c}{2187\sqrt{3}} - \frac{103t_c^2}{118098} + \frac{317t_c^3}{354294\sqrt{3}} - \frac{254887t_c^4}{1033121304} + \frac{8144183t_c^5}{46490458680\sqrt{3}} + \dots, \\ \Delta^z(t_c) &= -\frac{t_c}{324} + \frac{53t_c^2}{11664\sqrt{3}} - \frac{817t_c^3}{629856} + \frac{346487t_c^4}{408146688\sqrt{3}} - \frac{17312837t_c^5}{110199605760} + \dots \end{aligned} \quad (4.33)$$

Observe that while the coordinate rescaling  $t_c \rightarrow \sqrt{3}t_c$  can be used to make the expansions of (the closed string quantities)  $z(t_c)$  and  $S^{zz}(t_c)$  rational, the open string quantity  $\Delta^z(t_c)$  stays irrational, therefore in comparison to the oriented closed string case, we do not perform such a rescaling. (Although, the rescaling would still make the expansion of the amplitudes with an even number of boundaries rational.) Using these expansions, we obtain the following conifold expansions of the amplitudes given

above.

$$\begin{aligned}
\mathcal{F}^{(2,1)} &= -\frac{7}{466560\sqrt{3}} + \frac{1621t_c}{22394880} - \frac{97207t_c^2}{906992640\sqrt{3}} + \frac{18202763t_c^3}{587731230720} - \frac{71727601t_c^4}{3526387384320\sqrt{3}} + \dots, \\
\mathcal{F}^{(2,2)} &= -\frac{227t_c}{1492992\sqrt{3}} + \frac{954653t_c^2}{8707129344} - \frac{5012287t_c^3}{39182082048\sqrt{3}} + \frac{4892098657t_c^4}{135413275557888} + \dots, \\
\mathcal{F}^{(2,3)} &= \frac{545t_c}{8957952} - \frac{15095299t_c^2}{87071293440\sqrt{3}} + \frac{4878199531t_c^3}{56422198149120} - \frac{92953690463t_c^4}{1015599566684160\sqrt{3}} + \dots, \\
\mathcal{F}^{(2,4)} &= -\frac{2735t_c}{53747712\sqrt{3}} + \frac{520278533t_c^2}{8358844170240} - \frac{6588078971t_c^3}{56422198149120\sqrt{3}} + \frac{1013092981t_c^4}{20061226008576} + \dots,
\end{aligned} \tag{4.34}$$

in the oriented sector and

$$\begin{aligned}
\mathcal{K}^{(2,0)} &= -\frac{27}{128t_c^2} - \frac{47}{13824} + \frac{191t_c}{279936\sqrt{3}} + \frac{17693t_c^2}{201553920} - \frac{41893t_c^3}{408146688\sqrt{3}} + \dots, \\
\mathcal{K}^{(2,1)} &= \frac{19}{9216\sqrt{3}} - \frac{15955t_c}{35831808} - \frac{12149t_c^2}{161243136\sqrt{3}} + \frac{29671433t_c^3}{313456656384} - \frac{54115555t_c^4}{626913312768\sqrt{3}} + \dots, \\
\mathcal{K}^{(2,2)} &= -\frac{1003}{2654208} + \frac{9529t_c}{17915904\sqrt{3}} - \frac{330943t_c^2}{7739670528} - \frac{10573571t_c^3}{104485552128\sqrt{3}} + \dots, \\
\mathcal{K}^{(2,3)} &= \frac{491}{2654208\sqrt{3}} - \frac{25373t_c}{161243136} + \frac{615487t_c^2}{5159780352\sqrt{3}} + \frac{280904809t_c^3}{30091839012864} + \dots, \\
\mathcal{K}^{(2,4)} &= -\frac{193}{7077888} + \frac{191993t_c}{1719926784\sqrt{3}} - \frac{74663195t_c^2}{1486016741376} + \frac{690070327t_c^3}{30091839012864\sqrt{3}} + \dots,
\end{aligned} \tag{4.35}$$

in the unoriented sector. We observe that the open string amplitudes are all regular and  $\mathcal{K}^{(g,0)}$  possesses similarly to  $\mathcal{F}^{(g,0)}$  a gap at the conifold. Namely, as  $t_c \rightarrow 0$ , the amplitudes are of the general form

$$\begin{aligned}
\mathcal{F}^{(g,0)} &= \frac{\Phi_g}{t_c^{2g-2}} + \mathcal{O}(t_c^0), \\
\mathcal{K}^{(g,0)} &= \frac{\Psi_g}{t_c^{2g-2}} + \mathcal{O}(t_c^0),
\end{aligned} \tag{4.36}$$

the important point being that except for the leading singularity, the coefficients of the other singular terms all vanish. Furthermore, the order of the leading singularity at the conifold (of the amplitudes without fixed holomorphic ambiguities) can be easily parameterized in terms of  $g$ . Since we expect that this structure of the amplitudes is general, the holomorphic ambiguities parameterized by (4.29) need to preserve this structure. Each vanishing coefficient imposes one condition on  $a_{\mathcal{F}/\mathcal{K}}^{(g,h)}$ , *i.e.*, fixes one coefficient  $a_i$ . Hence, we deduce that the conifold gives the following number of conditions which can be used to (partly) fix the ambiguities of the amplitudes:

$$\#_c = \begin{cases} 2g - 3 & \text{for } \mathcal{K}^{(g,0)} \\ 2g - 2 & \text{for } \mathcal{K}^{(g,h)} \text{ and } \mathcal{F}^{(g,1)} \\ 2g - 1 & \text{for } \mathcal{F}^{(g,h)} \text{ (} h > 1 \text{)} \end{cases}. \tag{4.37}$$

Nevertheless,  $\sim g$  conditions remain undetermined. In particular, the leading singularities of the Klein bottle amplitudes  $\mathcal{K}^{(g,0)}$  at the conifold, which we have denoted as  $\Psi_g$ , needs to be understood. We will briefly come back to this point below.

One might hope that the left-over conditions can be fixed via some additional systematics at the orbifold point. However, performing similarly as above the expansions of the amplitudes at the orbifold point, we have to conclude that there is no apparent such systematics which could aid in fixing the remaining ambiguities. Therefore, for the time being we have to rely on localization to fix the  $\sim g$  remaining conditions. With the data at hand, we have completely determined  $\mathcal{G}^{(\chi)}$  from the individual amplitudes up to  $\chi = 6$ .

If we instead directly compute the combined amplitude  $\mathcal{G}^{(\chi)}$  via (4.20), we can go a bit further since the real topological vertex provides data for higher  $\chi$ . Similarly as for the individual amplitudes, we parameterize the holomorphic ambiguity of  $\mathcal{G}^{(\chi)}$  via

$$a_{\mathcal{G}}^{(\chi)} = \sum_{i=0}^n a_i \frac{z^{i+\delta}}{(1-27z)^\zeta}, \quad (4.38)$$

with  $n = \frac{3}{2}\zeta$ ,  $\delta = (\chi \bmod 2)/2$  and

$$\zeta = \begin{cases} \chi & \text{for } \chi \text{ even} \\ \chi - 1 & \text{for } \chi \text{ odd} \end{cases}. \quad (4.39)$$

The conifold expansion shows that  $\mathcal{G}^{(\chi)}$  possesses a gap for  $\chi$  even and is regular for  $\chi$  odd (this is as expected from the behavior of the individual amplitudes  $\mathcal{F}$  and  $\mathcal{K}$  at the conifold described above). Similarly as for the individual amplitudes  $\mathcal{F}$  and  $\mathcal{K}$ , we can easily deduce that the gap leads to

$$\#_c = \begin{cases} \chi - 1 & \text{for } \chi \text{ even} \\ \chi & \text{for } \chi \text{ odd} \end{cases}, \quad (4.40)$$

conditions to fix the  $(n+1)$  coefficients  $a_i$  of  $a_{\mathcal{G}}^{(\chi)}$  (if one can understand  $\Psi_g$ , the conifold gives exactly  $\chi$  conditions). Using the data from the real topological vertex given in table 4 of appendix A, we can fix the left-over conditions for some higher  $\chi$  and in this way completely determined the amplitudes  $\mathcal{G}^{(\chi)}$  up to  $\chi = 9$ .<sup>3</sup> The resulting real Gopakumar-Vafa invariants are listed in table 2 and 3 in appendix A.

Finally, let us spend a few words on the leading singularity of the  $\mathcal{K}^{(g,0)}$  at the conifold (4.36). It is well known that the coefficient of the leading singularity of the oriented closed string amplitudes  $\mathcal{F}^{(g,0)}$  at the conifold is given by [27, 28]

$$\Phi_g = \frac{B_{2g}}{2g(2g-2)}, \quad (4.41)$$

---

<sup>3</sup>The data at hand is sufficient to go up to  $\chi = 12$ .

$g$	1	2	3	4	5	6
$\Psi_g$	$-\frac{1}{8} \log(t_c)$	$-\frac{9}{128}$	$\frac{81}{512}$	$-\frac{4239}{4096}$	$\frac{221859}{16384}$	$-\frac{48938499}{163840}$

**Table 1:**  $\Psi_g$  for low  $g$  (note that we have rescaled  $t_c \rightarrow \sqrt{3}t_c$ ).

where  $B_{2g}$  are the Bernoulli numbers. The universality of the relationship (4.41) has been understood from many perspectives over the years. Among other things,  $\Phi_g$  gives the Euler characteristic of the moduli space of genus  $g$  complex curves. The gap structure was discovered in [15, 16], and explained physically in terms of the existence of a single light BPS state associated with the vanishing period at the conifold [29]. It behooves us to ask for a similar interpretation of the gap structure in  $\mathcal{K}^{(g,0)}$ . The coefficients  $\Psi_g$  have a good chance of being equally universal as the  $\Phi_g$ . For future reference, we list the values of  $\Psi_g$  for low  $g$  in table 1 and leave a detailed understanding to subsequent work. Note that  $\Psi_g$  can be conveniently extracted from  $\mathcal{G}^{(x)}$ , as defined in (1.9), expanded at the conifold point. This can be easily inferred from (1.3) combined with the regularity of the individual amplitudes with boundaries at the conifold point.

## 5 Conclusion

In this paper, we have initiated a detailed study of the real topological string on local Calabi-Yau threefolds. Whereas the topological string on local (toric) Calabi-Yaus (with toric branes) is essentially solved, and understood from a variety of different perspectives, and we have made significant progress on the systematics of the real topological string, much remains to be understood (both in the local and the compact situation). We see possibilities for further work in several directions.

The most interesting question to us is whether it is possible to achieve full integrability in the B-model, as is the case for the local closed topological string. As discussed in section 4.2, the behavior of the real amplitudes at the conifold point in moduli space does not yield enough constraints to fully fix the holomorphic ambiguities. Therefore, it would be very desirable to find additional systematic constraints in order to completely fix those ambiguities. A related question is the interpretation of the leading singularity of the Klein bottle amplitudes (without boundaries) at the conifold point. One expects to be able to find a closed expression for the leading coefficient and thereby obtain an additional constraint which aids in fixing the ambiguities.

Another possible line to follow would be to generalize the real topological vertex presented in section 3 to arbitrary local toric Calabi-Yau 3-folds. This would put the real topological string on equal footing with the closed topological string (for local geometries) and would open up the arena for various case studies and further investigations. One might also try to generalize the recent progress on spectral curve methods (see [31] for a review and references) as a B-model version of the topological vertex, to the real topological string. The explicit data obtained in this work should be helpful as guideline to find the right formulation.

Finally, from a mathematical point of view, the localization technique originally sketched in [30, 3], and reviewed and applied in section 2.2, needs to be formulated in a more rigorous way (especially the tadpole cancellation). Also, in order to put the enumerative aspects of the real topological string on a firmer mathematical ground, one should seek a proper definition of real Gopakumar-Vafa invariants.

We believe that with the present work in hand, the real topological string can indeed be put on equal footing with the topological string on local geometries in the near future. The compact case on the other hand might remain as a challenge for some time to come. The localization and topological vertex techniques are not applicable in the compact setting at higher genus. On the other hand, it is reasonable to expect that the gap structure that we found at the conifold will persist in compact models. This should allow for their solution to much higher level than before. Ultimately, progress on the open sector should also feed back to the closed topological string. So perhaps in combination, one can learn enough to solve both simultaneously. We look forward to further research on these matters.

**Acknowledgments** We like to thank the organizers of the sixth Simons workshop in Mathematics and Physics, where this work has been initiated, for ensuring a stimulating atmosphere. The work of D.K. was supported in part by an EU Marie-Curie EST fellowship.

## A Real Gopakumar-Vafa invariants of local $\mathbb{P}^2$

In this appendix, we list some real Gopakumar-Vafa invariants  $N_d^{(\chi)}$  of local  $\mathbb{P}^2$ . The results from the three complementary schemes that we have used all agree as far as we have checked.



$d \setminus \chi$	-1	0	1	2	3	4
1	$1^\diamond$		$0^*$		$0^*$	
2		$0^*$		$0^*$		$0^*$
3	$-1^\diamond$		$0^*$		$0^*$	
4		$3^*$		$1^*$		$0^*$
5	$5^\diamond$		$10^*$		$6^*$	
6		$-44^*$		$-63^*$		$-37^*$
7	$-42^\diamond$		$-229^*$		$-474^*$	
8		$675^*$		$2826^*$		$6641^*$
9	$429^\diamond$		$4833^*$		$24547^*$	
10		$-10596^*$		$-91309^*$		$-444825^*$
11	$-4939^\diamond$		$-96823^*$		$-922904^\diamond$	
12		$169815^\diamond$		$2548446^\diamond$		$22222821^\diamond$
13	$61555$		$1890640^\diamond$		$29568178^\diamond$	
14		$-2766312^\diamond$		$-65141982^\diamond$		$-907236837^\diamond$
15	$-811445$		$-36355693$		$-855398125$	
16		$45651033$		$1571061879$		$32383098135$
17	$11154329$		$692134092$		$23061556312$	
18		$-761270252$		$-36357840387$		$-1049953473666$
19	$-158387705$		$-13085426739$		$-590387680935$	
20		$12804181968$		$815896308217$		$31671654196277$
21	$2308018713$		$246141639751$		$14527282829907$	
22		$216905448900$		$-17878517912137$		$-903161239605882$
23	$-34350229129$		$-4612322986757$		$-346447571899667$	
24		$3696709999475$		$384413718899808$		$24622104921447319$
25	$520291543850$		$86171027900880$		$8055204030496600$	
26		$-63329911074864$		$-8138918187959256$		$-646992872220979059$
27	$-7998433661880$		$-1606102217387496$		$-183404890744633392$	
28		$1089804320192328$		$170128830773159693$		$16487461934782290071$
29	$124530193132562$		$29877825751921400$		$4102926664405466446$	
30		$-18827327577603608$		$-3518103635914287426$		$-409393336266808069759$

**Table 2:**  $N_d^{r(\chi)}$  for high  $d$  obtained from the B-model (numbers marked with  $\diamond$  have been verified via the real topological vertex, numbers marked with  $*$  in addition via localization).

$d \setminus \chi$	5	6	7	8	9
1	0*		0*		0*
2		0*		0*	
3	0*		0*		0*
4		0*		0*	
5	1*		0*		0*
6		-10*		-1*	
7	-497*		-286*		-91 $\diamond$
8		9688*		9909 $\diamond$	
9	76685*		162007 $\diamond$		240214 $\diamond$
10		-1490889 $\diamond$		-3622074 $\diamond$	
11	-5689826 $\diamond$		-24839317 $\diamond$		-80024538 $\diamond$
12		138741207 $\diamond$		660614879 $\diamond$	
13	309836946 $\diamond$		2387676377 $\diamond$		14155255239 $\diamond$
14		-9250663299 $\diamond$		-73688144692 $\diamond$	
15	-13813050354		-167924131768		-1606774464538
16		496417243815		6048297221530	
17	536811735677		9568553947097		136513807781008
18		-22814962465032		-399056811636330	
19	-18866208478280		-467697511728963		-9398297970384222
20		933580323856212		22370764847588270	
21	613983765096754		20339969314765719		551685003357975980
22		-34902135604573377		-1105187697763665228	
23	-18804234985799241		-806808827756109811		-28574033239468010587
24		1213849008767132251		49357611086785857295	
25	548264953334411255		29708534211072505345		1337857466210942972595
26		-39792028380461566548		-2029790874827662119329	
27	-15348471706637436099		-1028783168774451701259		-57640797365862616605714
28		1241733288505925189151		77934424856611454475555	
29	415237415601455194036		33835984504174543688472		231619419544332049565232
30		-37166974728897157340684		-2823578149528246194259586	

**Table 3:**  $N_d^{r(\chi)}$  for high  $d$  obtained from the B-model (numbers marked with  $\diamond$  have been verified via the real topological vertex, numbers marked with \* in addition via localization).

$\chi \setminus d$	6	7	8	9	10	11	12	13	14
10			6882		-6527094		2470331689		-472060307393
11		-15		254935		-195123249		66336579865	
12			3214		-8853482		7384195595		-2473627288265
13		-1		195943		-366754317		250379339074	
14			988		-9136211		17862370096		-10728530219814
15				109614		-539107092		771890474372	
16			191		-7226144		35296981346		-38871359145408
17				44507		-626854392		1965636872695	
18			21		-4398773		57410786270		-118572379592483
19				12949		-581661131		4173449453891	
20			1		-2061527		77347818109		-306601937181157
21				2626		-433433895		7446682383581	
22					-740639		86771638286		-676198602671642
23				352		-260366065		11241439498902	
24					-201867		81398541770		-1279073229693409
25				28		-126238105		14438862544045	
26					-40953		64054115660		-2085518321405375
27				1		-49322461		15854057302183	
28					-5985		42371627534		-2944249848639372
29						-15453034		14938241580054	
30					-595		23582667480		-3613212254655871
31						-3847413		12114187918765	
32					-36		11038869636		-3867758515991016
33						-750175		8473209466017	
34					-1		4337601572		-3621885665305630
35						-111971		5118273430606	
36							1425576149		-2974100596675286
37						-12342		2671254703769	
38							389623263		-2145509291350998
39						-946		1204005379440	
40							87807601		-1361557832849019
41						-45		467997216591	
42							16121003		-760697816260927
43						-1		156480858834	
44							2369885		-374239613900020
45								44835729183	
46							272051		-162059929797276
47								10949573048	
48							23479		-61706256970277
49								2262530362	
50							1432		-20621959046012
51								391668488	
52							55		-6032986939113
53								56047228	
54							1		-1539443942273
55								6508822	
56									-340986604623
57								597618	
58									-65152049938
59								41728	
60									-10651137069
61								2081	
62									-1474076916
63								66	
64									-170289956
65								1	
66									-16111390
67									
68									-1215524
69									
70									-70301
71									
72									-2926
73									
74									-78
75									
76									-1
77									

**Table 4:**  $N'_d(\chi)$  for high  $\chi$  obtained via the real topological vertex.

## References

- [1] A. Neitzke and C. Vafa, “Topological strings and their physical applications,” arXiv:hep-th/0410178.
- [2] M. Marino, “Chern-Simons theory and topological strings,” Rev. Mod. Phys. **77** (2005) 675 [arXiv:hep-th/0406005].
- [3] J. Walcher, “Evidence for Tadpole Cancellation in the Topological String,” arXiv:0712.2775 [hep-th].
- [4] H. Ooguri and C. Vafa, “Knot invariants and topological strings,” Nucl. Phys. B **577**, 419 (2000) [arXiv:hep-th/9912123].
- [5] M. Kontsevich, “Enumeration Of Rational Curves Via Torus Actions,” arXiv:hep-th/9405035.
- [6] T. Graber and E. Zaslow, “Open string Gromov-Witten invariants: Calculations and a mirror ‘theorem’,” arXiv:hep-th/0109075.
- [7] D. E. Diaconescu, B. Florea and A. Misra, “Orientifolds, unoriented instantons and localization,” JHEP **0307** (2003) 041 [arXiv:hep-th/0305021].
- [8] A. Klemm and E. Zaslow, “Local mirror symmetry at higher genus,” arXiv:hep-th/9906046.
- [9] P. Mayr, “Summing up open string instantons and  $N = 1$  string amplitudes,” arXiv:hep-th/0203237.
- [10] M. Aganagic, A. Klemm, M. Marino and C. Vafa, “The topological vertex,” Commun. Math. Phys. **254** (2005) 425 [arXiv:hep-th/0305132].
- [11] V. Bouchard, B. Florea and M. Marino, “Counting higher genus curves with crosscaps in Calabi-Yau orientifolds,” JHEP **0412** (2004) 035 [arXiv:hep-th/0405083].
- [12] V. Bouchard, B. Florea and M. Marino, “Topological open string amplitudes on orientifolds,” JHEP **0502** (2005) 002 [arXiv:hep-th/0411227].
- [13] M. Bershadsky, S. Cecotti, H. Ooguri and C. Vafa, “Kodaira-Spencer theory of gravity and exact results for quantum string amplitudes,” Commun. Math. Phys. **165** (1994) 311 [arXiv:hep-th/9309140].
- [14] J. Walcher, “Extended Holomorphic Anomaly and Loop Amplitudes in Open Topological String,” arXiv:0705.4098 [hep-th].
- [15] M. x. Huang and A. Klemm, “Holomorphic anomaly in gauge theories and matrix models,” JHEP **0709** (2007) 054 [arXiv:hep-th/0605195].
- [16] M. x. Huang, A. Klemm and S. Quackenbush, “Topological String Theory on Compact Calabi-Yau: Modularity and Boundary Conditions,” arXiv:hep-th/0612125.
- [17] B. Haghighat, A. Klemm and M. Rauch, “Integrability of the holomorphic anomaly equations,” JHEP **0810** (2008) 097 [arXiv:0809.1674 [hep-th]].

- [18] T. Graber and R. Pandharipande, “Localization of Virtual Classes,” arXiv:math.ag/9708001.
- [19] C. Faber, “Algorithm for Computing Intersection Numbers on Moduli Spaces of Curves, with an Application to the Class of the Locus of the Jacobians,” arXiv:math.ag/9706006.
- [20] R. Pandharipande, J. Solomon and J. Walcher, “Disk enumeration on the quintic 3-fold,” arXiv:math.sg/0610901.
- [21] M. Aganagic, M. Marino and C. Vafa, “All loop topological string amplitudes from Chern-Simons theory,” Commun. Math. Phys. **247**, 467 (2004) [arXiv:hep-th/0206164].
- [22] A. Iqbal, “All genus topological string amplitudes and 5-brane webs as Feynman diagrams,” arXiv:hep-th/0207114.
- [23] D. E. Diaconescu and B. Florea, “Localization and gluing of topological amplitudes,” Commun. Math. Phys. **257**, 119 (2005) [arXiv:hep-th/0309143].
- [24] S. Yamaguchi and S. T. Yau, “Topological string partition functions as polynomials,” JHEP **0407** (2004) 047 [arXiv:hep-th/0406078].
- [25] Y. Konishi and S. Minabe, “On Solutions to Walcher’s holomorphic anomaly equations,” arXiv:0708.2898 [math.AG]
- [26] M. Alim and J. D. Lange, “Polynomial Structure of the (Open) Topological String Partition Function,” JHEP **0710** (2007) 045 [arXiv:0708.2886 [hep-th]].
- [27] D. Ghoshal and C. Vafa, “C = 1 String As The Topological Theory Of The Conifold,” Nucl. Phys. B **453** (1995) 121 [arXiv:hep-th/9506122].
- [28] H. Ooguri and C. Vafa, “Worldsheet Derivation of a Large N Duality,” Nucl. Phys. B **641** (2002) 3 [arXiv:hep-th/0205297].
- [29] C. Vafa, “A Stringy test of the fate of the conifold,” Nucl. Phys. B **447**, 252 (1995) [arXiv:hep-th/9505023].
- [30] J. Walcher, “Opening mirror symmetry on the quintic,” Commun. Math. Phys. **276** (2007) 671 [arXiv:hep-th/0605162].
- [31] B. Eynard and N. Orantin, “Algebraic methods in random matrices and enumerative geometry,” arXiv:0811.3531 [math-ph].